Electronic Supplementary Material (ESI) for Physical Chemistry Chemical Physics

Supporting Information

How Ion Properties Determine the Stability of a Lipase Enzyme in Ionic Liquids: A Molecular Dynamics Study

Marco Klähn,* Geraldine S. Lim and Ping Wu

Institute of High Performance Computing, 1 Fusionopolis Way, #16-16, Connexis, Singapore 138632, Rep. of Singapore

* To whom correspondence should be addressed. Phone: (65) 6419 1468. Fax: (65) 6463 2536.

E-mail: marco@ihpc.a-star.edu.sg

Table S1 Change of Total, Coulomb and Lennard-Jones Interaction Strength between α–helix of CAL-B and IL, Cations and Anions after Partial Unfolding of CAL-B[a]

BMIM-PF_6				**BMIM-BF_4**			
	$\Delta E_{prot-IL}$	ΔE^{Coul}	ΔE^{LJ}		$\Delta E_{prot-IL}$	ΔE^{Coul}	ΔE^{LJ}
IL	-0.879	-0.475	-0.403	IL	-0.640	-0.289	-0.351
$BMIM^+$	-2.483	-2.170	-0.313	$BMIM^+$	-1.207	-0.895	-0.312
PF_6^-	1.604	1.695	-0.091	BF_4^-	0.567	0.606	-0.039
BMIM-NO_3				**MOEMIM-BF_4**			
	$\Delta E_{prot-IL}$	ΔE^{Coul}	ΔE^{LJ}		$\Delta E_{prot-IL}$	ΔE^{Coul}	ΔE^{LJ}
IL	-4.406	-3.147	-1.259	IL	-2.693	-2.020	-0.673
$BMIM^+$	2.207	3.176	-0.970	$MOEMIM^+$	2.237	2.800	-0.563
NO_3^-	-6.612	-6.323	-0.289	BF_4^-	-4.930	-4.820	-0.110
MCGUA-NO_3				**BCGUA-BF_4**			
	$\Delta E_{prot-IL}$	ΔE^{Coul}	ΔE^{LJ}		$\Delta E_{prot-IL}$	ΔE^{Coul}	ΔE^{LJ}
IL	-2.670	-1.820	-0.850	IL	-0.829	-0.273	-0.556
$MCGUA^+$	2.445	3.119	-0.674	$BCGUA^+$	0.781	1.267	-0.486
NO_3^-	-5.116	-4.940	-0.176	BF_4^-	-1.610	-1.540	-0.071
DCGUA-NO_3				**BAGUA-BF_4**			
	$\Delta E_{prot-IL}$	ΔE^{Coul}	ΔE^{LJ}		$\Delta E_{prot-IL}$	ΔE^{Coul}	ΔE^{LJ}
IL	-2.492	-1.445	-1.047	IL	-0.664	-0.068	-0.596
$DCGUA^+$	-0.065	0.845	-0.910	$BAGUA^+$	-0.884	-0.368	-0.516
NO_3^-	-2.427	-2.290	-0.137	BF_4^-	0.219	0.300	-0.080

[a] Interaction changes were calculated as differences between the initial α-helix-solvent interaction strength and after an MD simulation of 5 ns length at 600 K. Energies are given in MJ/mol, where negative values correspond to increasing interaction strengths after partial protein unfolding. Together with the total interaction changes, contributions from Coulomb and Lennard-Jones potential, as well as from cations and anions, are given separately.

Table S2 Change of Total, Coulomb and Lennard-Jones Interaction Strength between β–sheet of CAL-B and IL, Cations and Anions after Partial Unfolding of CAL-B[a]

BMIM-PF_6				**BMIM-BF_4**			
	$\Delta E_{prot-IL}$	ΔE^{Coul}	ΔE^{LJ}		$\Delta E_{prot-IL}$	ΔE^{Coul}	ΔE^{LJ}
IL	-0.148	-0.042	-0.106	IL	-0.281	-0.116	-0.165
$BMIM^+$	0.626	0.694	-0.068	$BMIM^+$	2.011	2.142	-0.131
PF_6^-	-0.774	-0.736	-0.038	BF_4^-	-2.292	-2.258	-0.035
BMIM-NO_3				**MOEMIM-BF_4**			
	$\Delta E_{prot-IL}$	ΔE^{Coul}	ΔE^{LJ}		$\Delta E_{prot-IL}$	ΔE^{Coul}	ΔE^{LJ}
IL	-1.064	-0.803	-0.261	IL	-0.379	-0.185	-0.194
$BMIM^+$	1.362	1.561	-0.199	$MOEMIM^+$	2.180	2.348	-0.168
NO_3^-	-2.426	-2.364	-0.062	BF_4^-	-2.559	-2.534	-0.026
MCGUA-NO_3				**BCGUA-BF_4**			
	$\Delta E_{prot-IL}$	ΔE^{Coul}	ΔE^{LJ}		$\Delta E_{prot-IL}$	ΔE^{Coul}	ΔE^{LJ}
IL	-0.698	-0.445	-0.254	IL	-0.558	-0.389	-0.169
$MCGUA^+$	3.769	3.957	-0.188	$BCGUA^+$	2.582	2.730	-0.148
NO_3^-	-4.467	-4.402	-0.066	BF_4^-	-3.140	-3.119	-0.021
DCGUA-NO_3				**BAGUA-BF_4**			
	$\Delta E_{prot-IL}$	ΔE^{Coul}	ΔE^{LJ}		$\Delta E_{prot-IL}$	ΔE^{Coul}	ΔE^{LJ}
IL	-0.216	0.096	-0.312	IL	0.106	0.166	-0.060
$DCGUA^+$	1.763	2.015	-0.252	$BAGUA^+$	3.621	3.662	-0.041
NO_3^-	-1.979	-1.919	-0.060	BF_4^-	-3.515	-3.496	-0.018

[a] Interaction changes were calculated as differences between the initial β-sheet-solvent interaction strength and after an MD simulation of 5 ns length at 600 K. Energies are given in MJ/mol, where negative values correspond to increasing interaction strengths after partial protein unfolding. Together with the total interaction changes, contributions from Coulomb and Lennard-Jones potential, as well as from cations and anions, are given separately.

Table S3 Change of Total, Coulomb and Lennard-Jones Interaction Strength between turn/coil of CAL-B and IL, Cations and Anions after Partial Unfolding of CAL-B[a]

BMIM-PF_6				**BMIM-BF_4**			
	$\Delta E_{prot-IL}$	ΔE^{Coul}	ΔE^{LJ}		$\Delta E_{prot-IL}$	ΔE^{Coul}	ΔE^{LJ}
IL	-3.029	-2.318	-0.711	IL	-3.246	-2.440	-0.806
$BMIM^+$	1.206	1.736	-0.530	$BMIM^+$	0.094	0.779	-0.685
PF_6^-	-4.234	-4.053	-0.181	BF_4^-	-3.341	-3.219	-0.121
BMIM-NO_3				**MOEMIM-BF_4**			
	$\Delta E_{prot-IL}$	ΔE^{Coul}	ΔE^{LJ}		$\Delta E_{prot-IL}$	ΔE^{Coul}	ΔE^{LJ}
IL	-5.181	-3.908	-1.273	IL	-3.506	-2.867	-0.639
$BMIM^+$	-8.913	-7.935	-0.978	$MOEMIM^+$	-0.841	-0.304	-0.537
NO_3^-	3.732	4.026	-0.294	BF_4^-	-2.665	-2.563	-0.102
MCGUA-NO_3				**BCGUA-BF_4**			
	$\Delta E_{prot-IL}$	ΔE^{Coul}	ΔE^{LJ}		$\Delta E_{prot-IL}$	ΔE^{Coul}	ΔE^{LJ}
IL	-5.037	-3.826	-1.211	IL	-3.215	-2.434	-0.781
$MCGUA^+$	-5.590	-4.646	-0.944	$BCGUA^+$	-0.072	0.610	-0.683
NO_3^-	0.553	0.819	-0.267	BF_4^-	-3.142	-3.044	-0.098
DCGUA-NO_3				**BAGUA-BF_4**			
	$\Delta E_{prot-IL}$	ΔE^{Coul}	ΔE^{LJ}		$\Delta E_{prot-IL}$	ΔE^{Coul}	ΔE^{LJ}
IL	-4.510	-3.190	-1.320	IL	-2.317	-1.676	-0.640
$DCGUA^+$	-2.658	-1.616	-1.043	$BAGUA^+$	-2.431	-1.893	-0.538
NO_3^-	-1.852	-1.574	-0.277	BF_4^-	0.114	0.217	-0.103

[a] Interaction changes were calculated as differences between the initial turn/coil-solvent interaction strength and after an MD simulation of 5 ns length at 600 K. Energies are given in MJ/mol, where negative values correspond to increasing interaction strengths after partial protein unfolding. Together with the total interaction changes, contributions from Coulomb and Lennard-Jones potential, as well as from cations and anions, are given separately.

Table S4 Initial Total, Coulomb and Lennard-Jones Interaction Strength between α–helix of CAL-B and IL, Cations and Anions[a]

BMIM-PF_6				**BMIM-BF_4**			
	$E_{0,prot-IL}$	$E^{0,Coul}$	$E^{0,LJ}$		$E_{0,prot-IL}$	$E^{0,Coul}$	$E^{0,LJ}$
IL	-3.288	-2.108	-1.180	IL	-4.130	-2.907	-1.222
$BMIM^+$	-5.938	-5.066	-0.872	$BMIM^+$	-5.929	-4.902	-1.027
PF_6^-	2.650	2.958	-0.308	BF_4^-	1.799	1.995	-0.196
BMIM-NO_3				**MOEMIM-BF_4**			
	$E_{0,prot-IL}$	$E^{0,Coul}$	$E^{0,LJ}$		$E_{0,prot-IL}$	$E^{0,Coul}$	$E^{0,LJ}$
IL	-4.034	-2.586	-1.448	IL	-3.372	-2.190	-1.183
$BMIM^+$	-6.808	-5.665	-1.143	$MOEMIM^+$	-6.804	-5.818	-0.986
NO_3^-	2.775	3.079	-0.305	BF_4^-	3.432	3.629	-0.197
MCGUA-NO_3				**BCGUA-BF_4**			
	$E_{0,prot-IL}$	$E^{0,Coul}$	$E^{0,LJ}$		$E_{0,prot-IL}$	$E^{0,Coul}$	$E^{0,LJ}$
IL	-3.901	-2.348	-1.552	IL	-3.691	-2.496	-1.195
$MCGUA^+$	-7.133	-5.946	-1.187	$BCGUA^+$	-6.041	-5.030	-1.011
NO_3^-	3.233	3.598	-0.365	BF_4^-	2.349	2.533	-0.184
DCGUA-NO_3				**BAGUA-BF_4**			
	$E_{0,prot-IL}$	$E^{0,Coul}$	$E^{0,LJ}$		$E_{0,prot-IL}$	$E^{0,Coul}$	$E^{0,LJ}$
IL	-3.893	-2.555	-1.338	IL	-2.934	-1.896	-1.038
$DCGUA^+$	-5.433	-4.315	-1.118	$BAGUA^+$	-4.622	-3.747	-0.875
NO_3^-	1.540	1.760	-0.220	BF_4^-	1.688	1.851	-0.163

[a] Energies are given in MJ/mol. Together with the total initial α-helix-IL interaction strength, contributions from Coulomb and Lennard-Jones potential, as well as from cations and anions, are given separately.

Table S5 Initial Total, Coulomb and Lennard-Jones Interaction Strength between β–sheet of CAL-B and IL, Cations and Anions[a]

BMIM-PF_6				**BMIM-BF_4**			
	$E_{0,prot-IL}$	$E^{0,Coul}$	$E^{0,LJ}$		$E_{0,prot-IL}$	$E^{0,Coul}$	$E^{0,LJ}$
IL	-1.641	-1.368	-0.273	IL	-1.656	-1.413	-0.243
$BMIM^+$	53.998	54.185	-0.187	$BMIM^+$	57.773	57.974	-0.202
PF_6^-	-55.639	-55.553	-0.086	BF_4^-	-59.429	-59.387	-0.042
BMIM-NO_3				**MOEMIM-BF_4**			
	$E_{0,prot-IL}$	$E^{0,Coul}$	$E^{0,LJ}$		$E_{0,prot-IL}$	$E^{0,Coul}$	$E^{0,LJ}$
IL	-1.702	-1.362	-0.339	IL	-1.336	-1.068	-0.268
$BMIM^+$	60.976	61.236	-0.260	$MOEMIM^+$	62.019	62.239	-0.220
NO_3^-	-62.677	-62.598	-0.079	BF_4^-	-63.355	-63.307	-0.048
MCGUA-NO_3				**BCGUA-BF_4**			
	$E_{0,prot-IL}$	$E^{0,Coul}$	$E^{0,LJ}$		$E_{0,prot-IL}$	$E^{0,Coul}$	$E^{0,LJ}$
IL	-1.625	-1.269	-0.356	IL	-1.419	-1.138	-0.281
$MCGUA^+$	76.582	76.848	-0.265	$BCGUA^+$	52.154	52.392	-0.238
NO_3^-	-78.207	-78.117	-0.090	BF_4^-	-53.573	-53.530	-0.043
DCGUA-NO_3				**BAGUA-BF_4**			
	$E_{0,prot-IL}$	$E^{0,Coul}$	$E^{0,LJ}$		$E_{0,prot-IL}$	$E^{0,Coul}$	$E^{0,LJ}$
IL	-1.877	-1.584	-0.293	IL	-1.152	-0.905	-0.247
$DCGUA^+$	39.651	39.897	-0.246	$BAGUA^+$	40.821	41.026	-0.205
NO_3^-	-41.528	-41.481	-0.047	BF_4^-	-41.973	-41.931	-0.042

[a] Energies are given in MJ/mol. Together with the total initial β-sheet-IL interaction strength, contributions from Coulomb and Lennard-Jones potential, as well as from cations and anions, are given separately.

Table S6 Initial Total, Coulomb and Lennard-Jones Interaction Strength between turn/coil of CAL-B and IL, Cations and Anions[a]

BMIM-PF_6				**BMIM-BF_4**			
	$E_{0,prot-IL}$	$E^{0,Coul}$	$E^{0,LJ}$		$E_{0,prot-IL}$	$E^{0,Coul}$	$E^{0,LJ}$
IL	-7.791	-5.227	-2.564	IL	-8.637	-6.027	-2.609
$BMIM^+$	-52.774	-50.882	-1.892	$BMIM^+$	-54.889	-52.713	-2.176
PF_6^-	44.983	45.654	-0.671	BF_4^-	46.253	46.686	-0.433
BMIM-NO_3				**MOEMIM-BF_4**			
	$E_{0,prot-IL}$	$E^{0,Coul}$	$E^{0,LJ}$		$E_{0,prot-IL}$	$E^{0,Coul}$	$E^{0,LJ}$
IL	-10.396	-7.234	-3.163	IL	-8.994	-6.303	-2.691
$BMIM^+$	-57.202	-54.742	-2.460	$MOEMIM^+$	-57.779	-55.572	-2.207
NO_3^-	46.806	47.509	-0.703	BF_4^-	48.785	49.269	-0.484
MCGUA-NO_3				**BCGUA-BF_4**			
	$E_{0,prot-IL}$	$E^{0,Coul}$	$E^{0,LJ}$		$E_{0,prot-IL}$	$E^{0,Coul}$	$E^{0,LJ}$
IL	-10.828	-7.406	-3.422	IL	-8.321	-5.699	-2.622
$MCGUA^+$	-73.433	-70.852	-2.581	$BCGUA^+$	-52.124	-49.915	-2.209
NO_3^-	62.605	63.446	-0.841	BF_4^-	43.804	44.217	-0.413
DCGUA-NO_3				**BAGUA-BF_4**			
	$E_{0,prot-IL}$	$E^{0,Coul}$	$E^{0,LJ}$		$E_{0,prot-IL}$	$E^{0,Coul}$	$E^{0,LJ}$
IL	-8.660	-5.850	-2.810	IL	-7.254	-4.914	-2.340
$DCGUA^+$	-39.985	-37.622	-2.363	$BAGUA^+$	-40.929	-38.960	-1.969
NO_3^-	31.324	31.772	-0.447	BF_4^-	33.675	34.047	-0.371

[a] Energies are given in MJ/mol. Together with the total initial turn/coil-IL interaction strength, contributions from Coulomb and Lennard-Jones potential, as well as from cations and anions, are given separately.

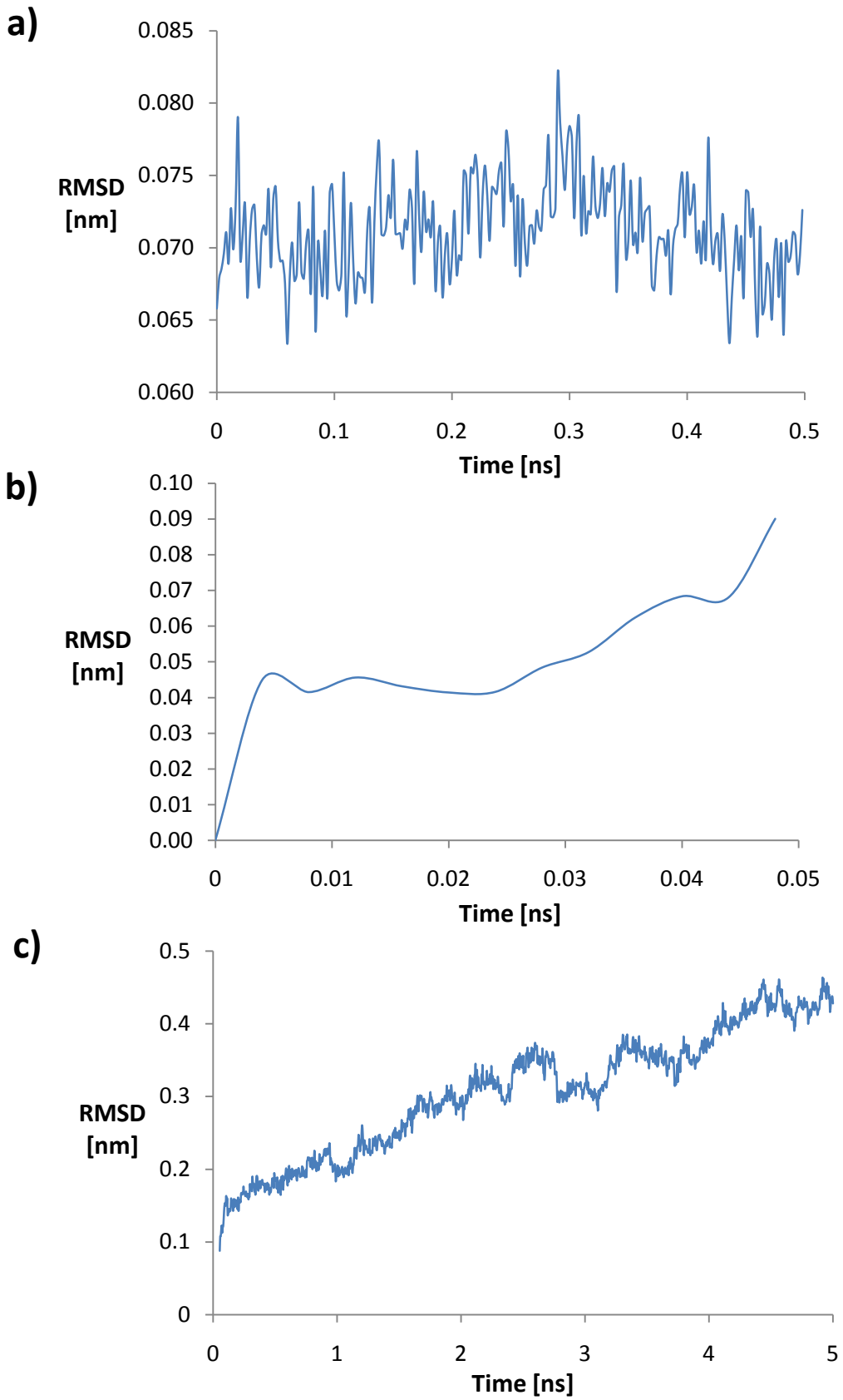

Fig. S1 Plot of root mean square deviation, RMSD, of CAL-B solvated by BMIM-PF_6 over time during a) the last 500 ps of the 300K MD simulation b) the 50 ps heating phase from 1 to 600K c) the 4.95 ns MD simulation at 600K.

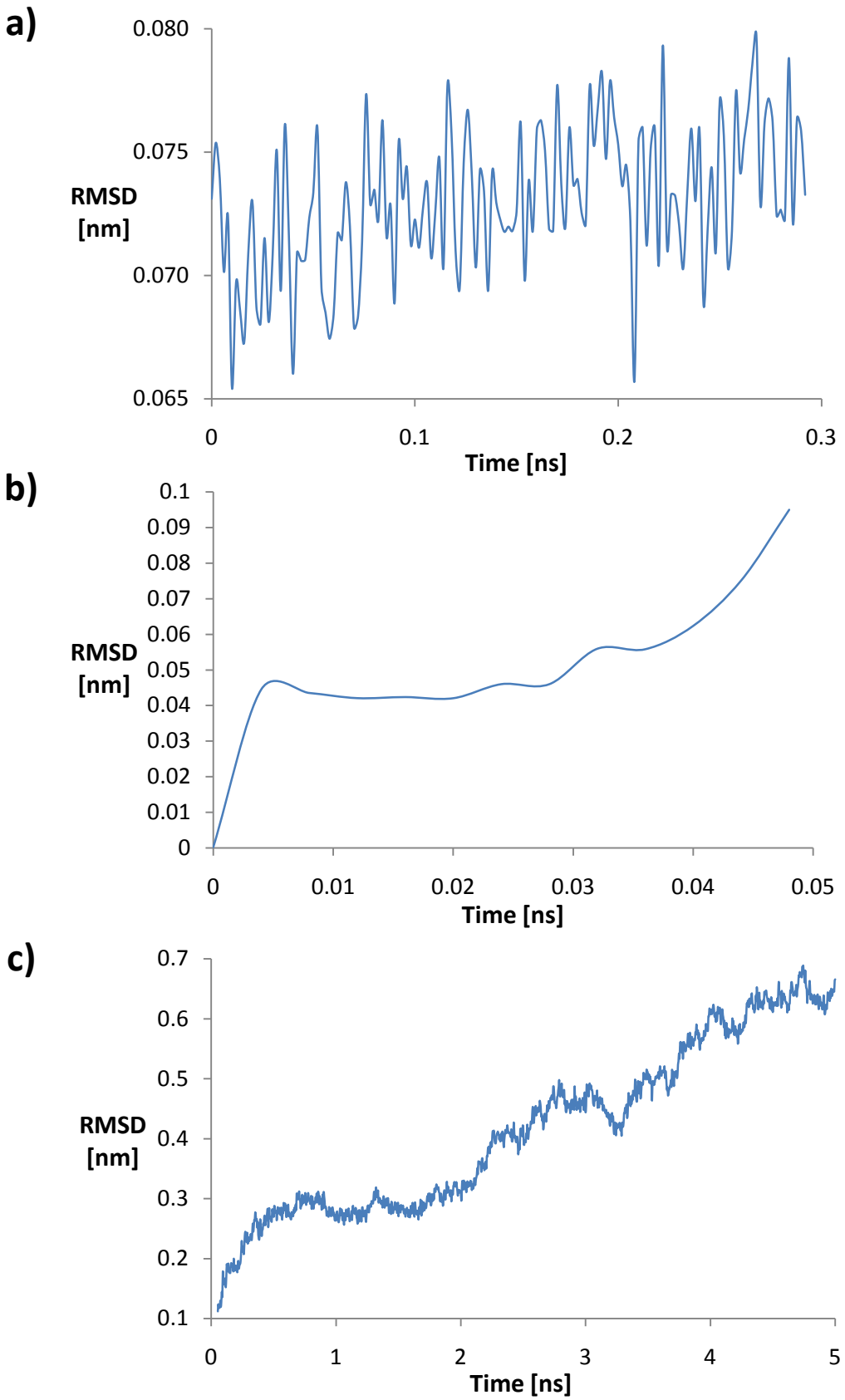

Fig. S2 Plot of root mean square deviation, RMSD, of CAL-B solvated by BMIM-NO_3 over time during a) the last 300 ps of the 300K MD simulation b) the 50 ps heating phase from 1 to 600K c) the 4.95 ns MD simulation at 600K.

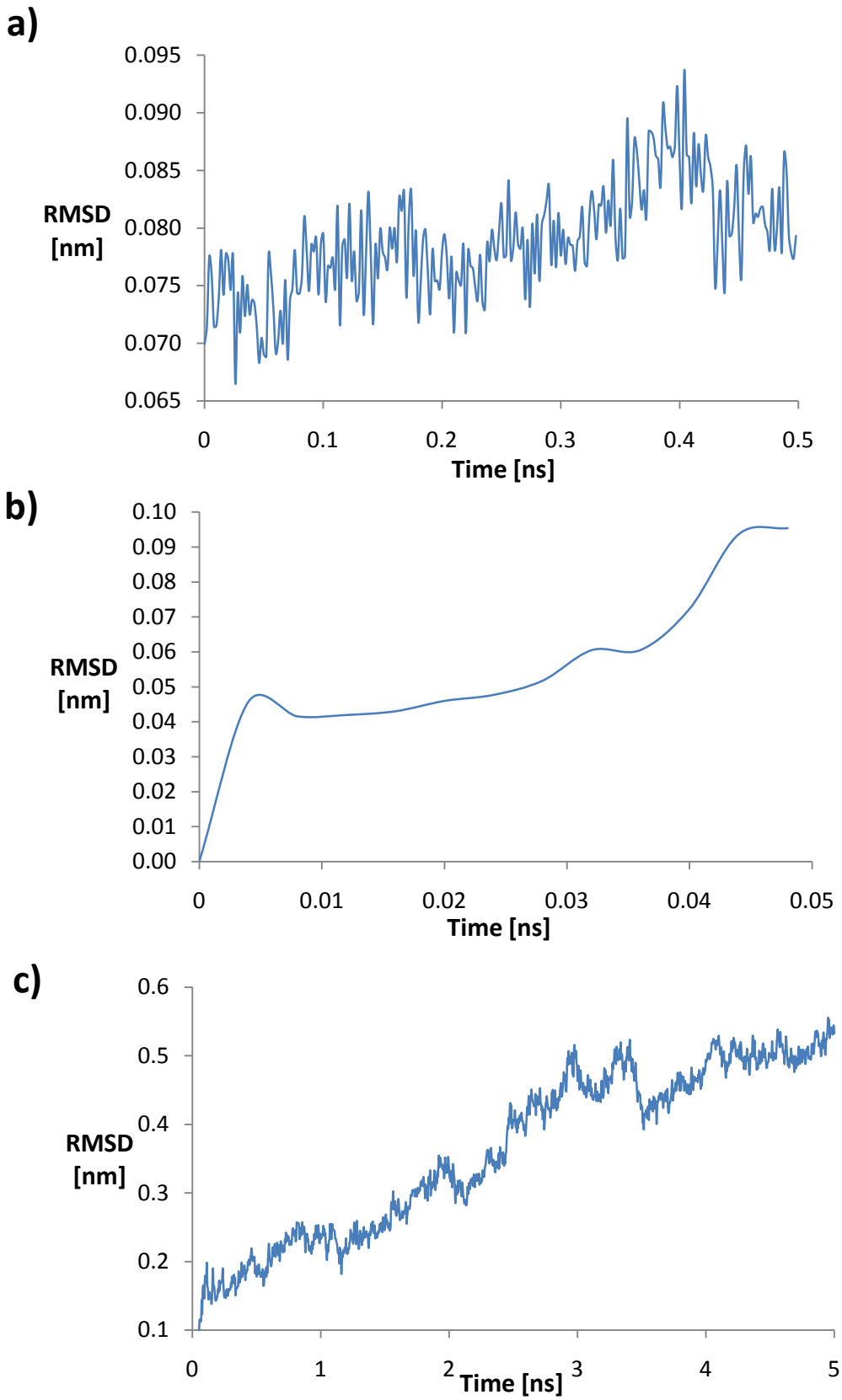

Fig. S3 Plot of root mean square deviation, RMSD, of CAL-B solvated by BMIM-BF_4 over time during a) the last 500 ps of the 300K MD simulation b) the 50 ps heating phase from 1 to 600K c) the 4.95 ns MD simulation at 600K.

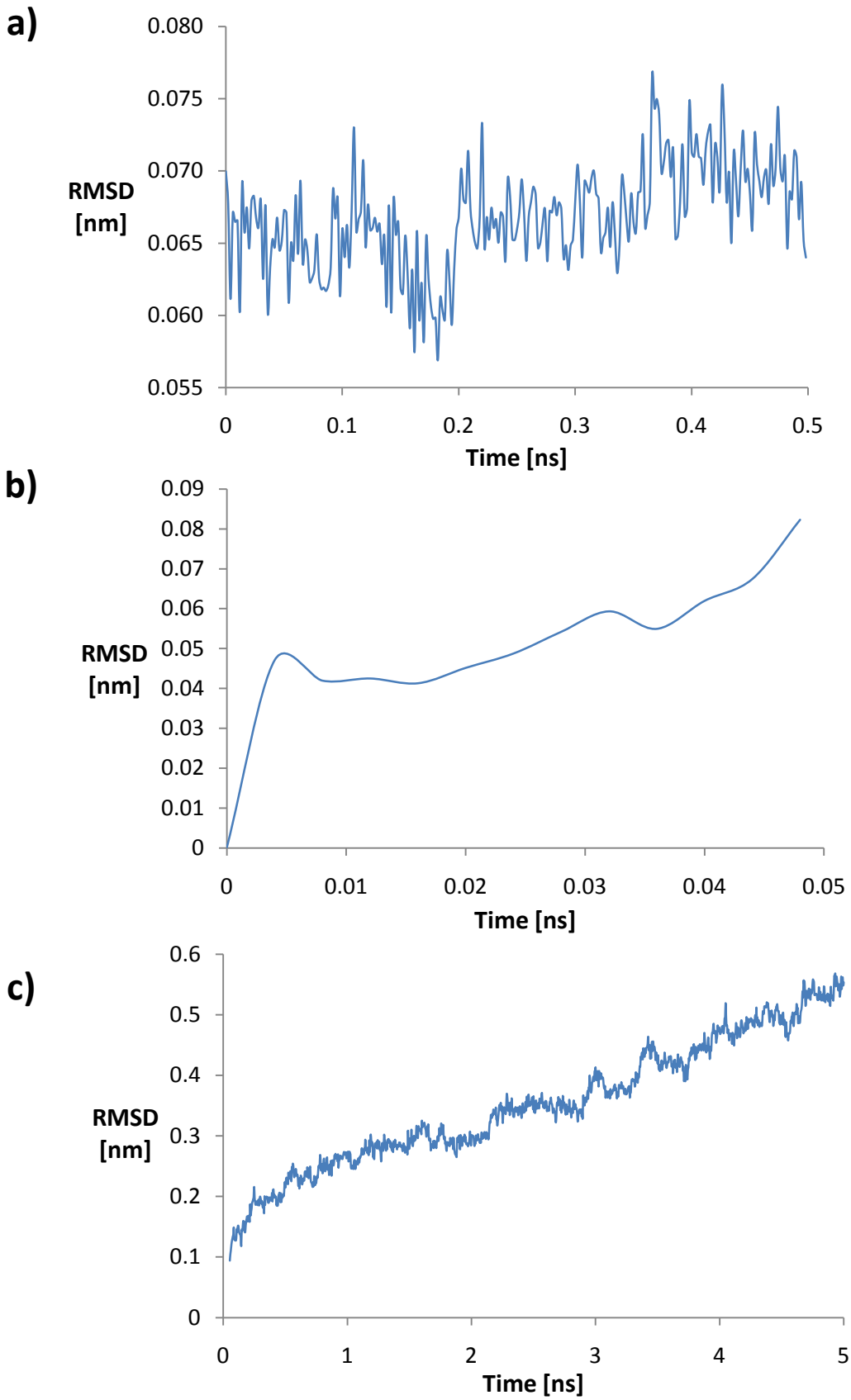

Fig. S4 Plot of root mean square deviation, RMSD, of CAL-B solvated by MOEMIM-BF_4 over time during a) the last 500 ps of the 300K MD simulation b) the 50 ps heating phase from 1 to 600K c) the 4.95 ns MD simulation at 600K.

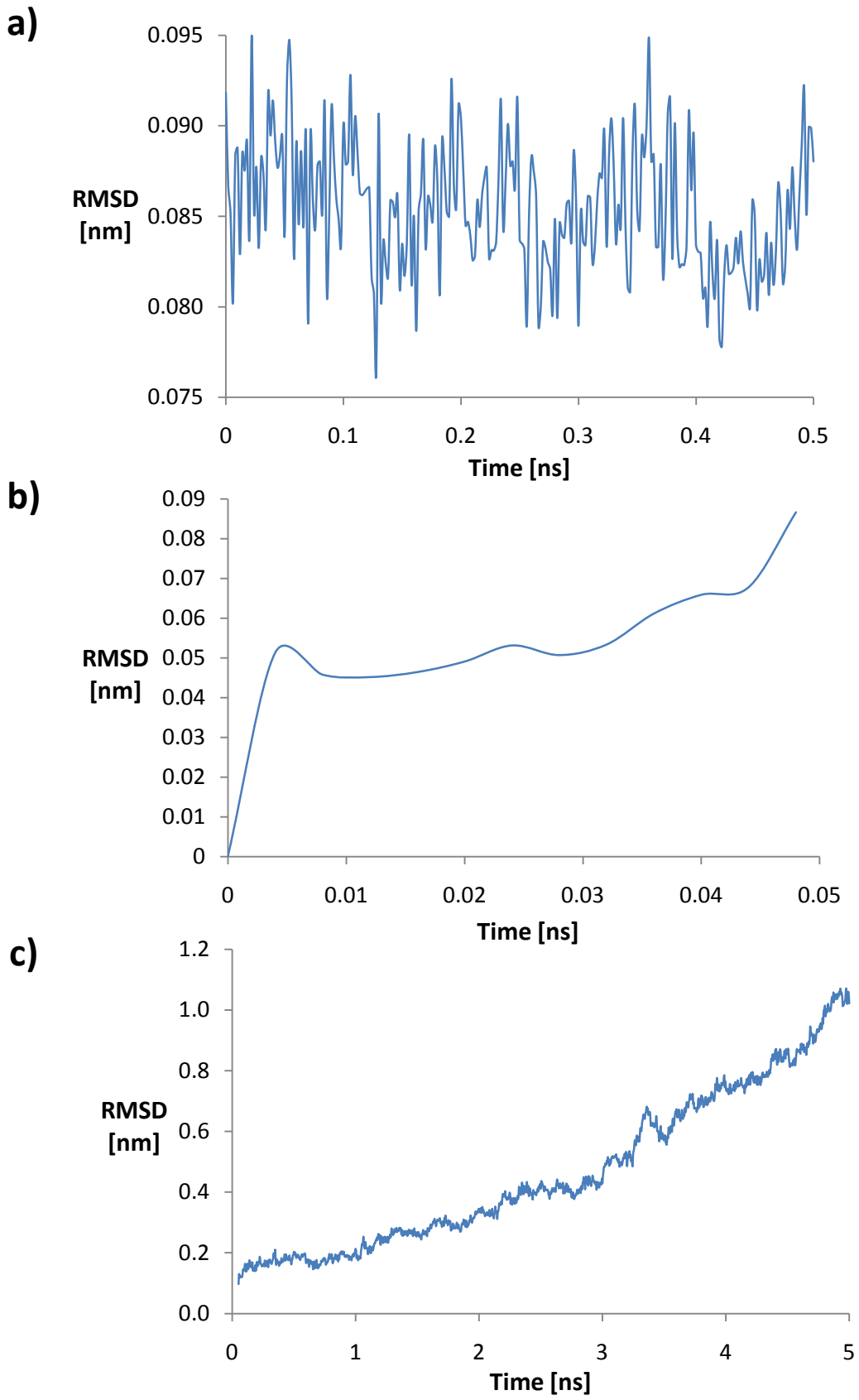

Fig. S5 Plot of root mean square deviation, RMSD, of CAL-B solvated by BAGUA-BF_4 over time during a) the last 500 ps of the 300K MD simulation b) the 50 ps heating phase from 1 to 600K c) the 4.95 ns MD simulation at 600K.

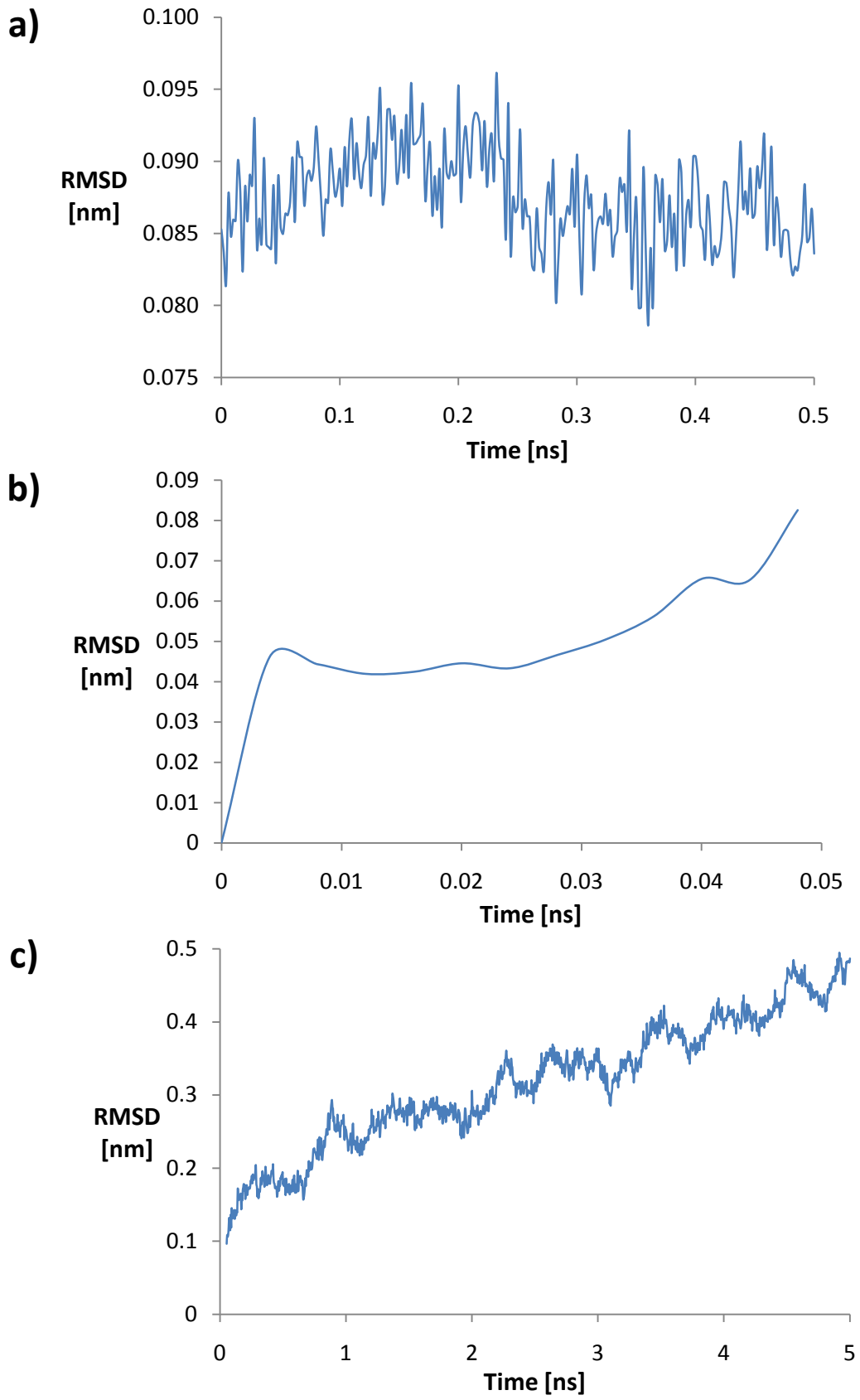

Fig. S6 Plot of root mean square deviation, RMSD, of CAL-B solvated by BCGUA-BF_4 over time during a) the last 500 ps of the 300K MD simulation b) the 50 ps heating phase from 1 to 600K c) the 4.95 ns MD simulation at 600K.

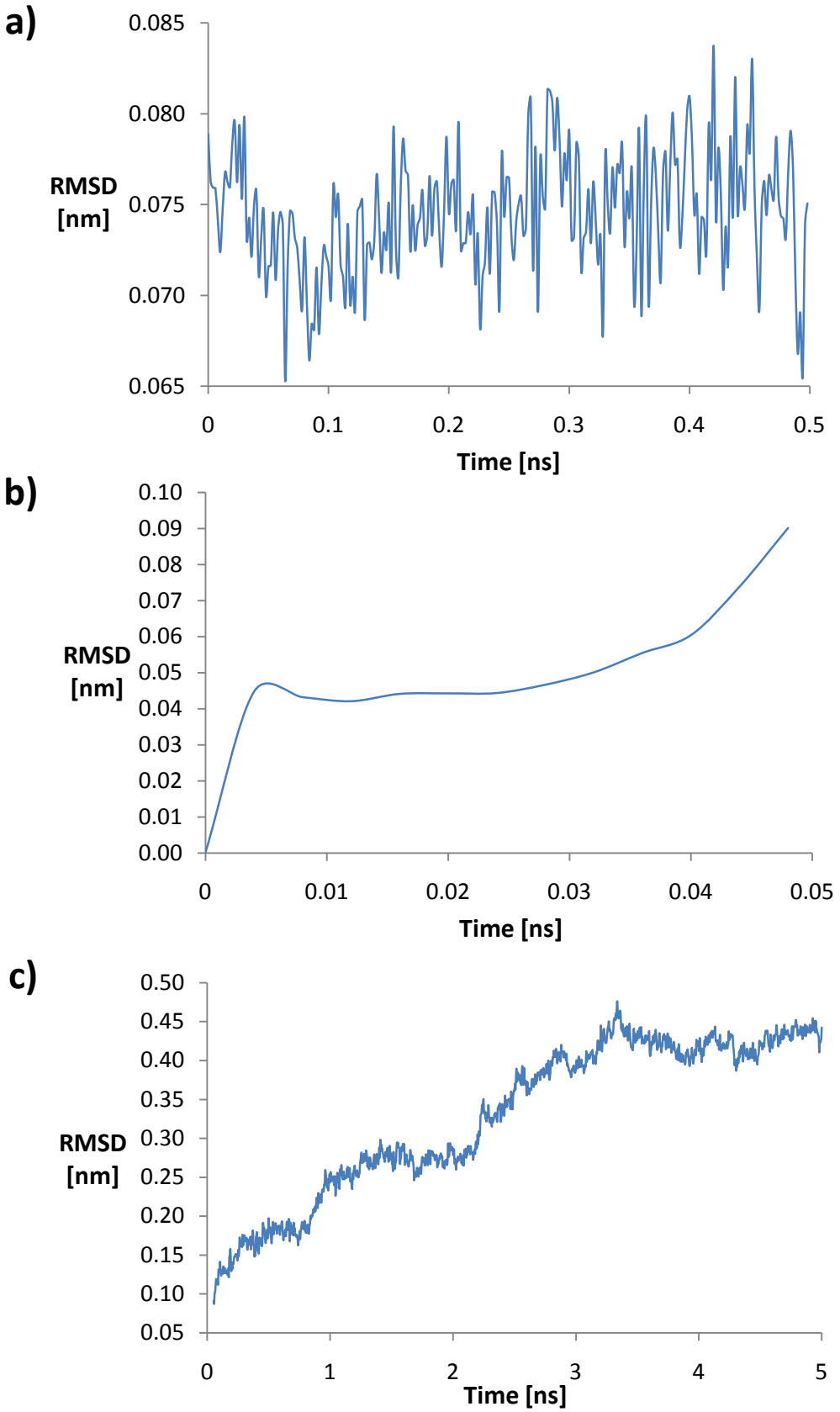

Fig. S7 Plot of root mean square deviation, RMSD, of CAL-B solvated by MCGUA-NO_3 over time during a) the last 500 ps of the 300K MD simulation b) the 50 ps heating phase from 1 to 600K c) the 4.95 ns MD simulation at 600K.

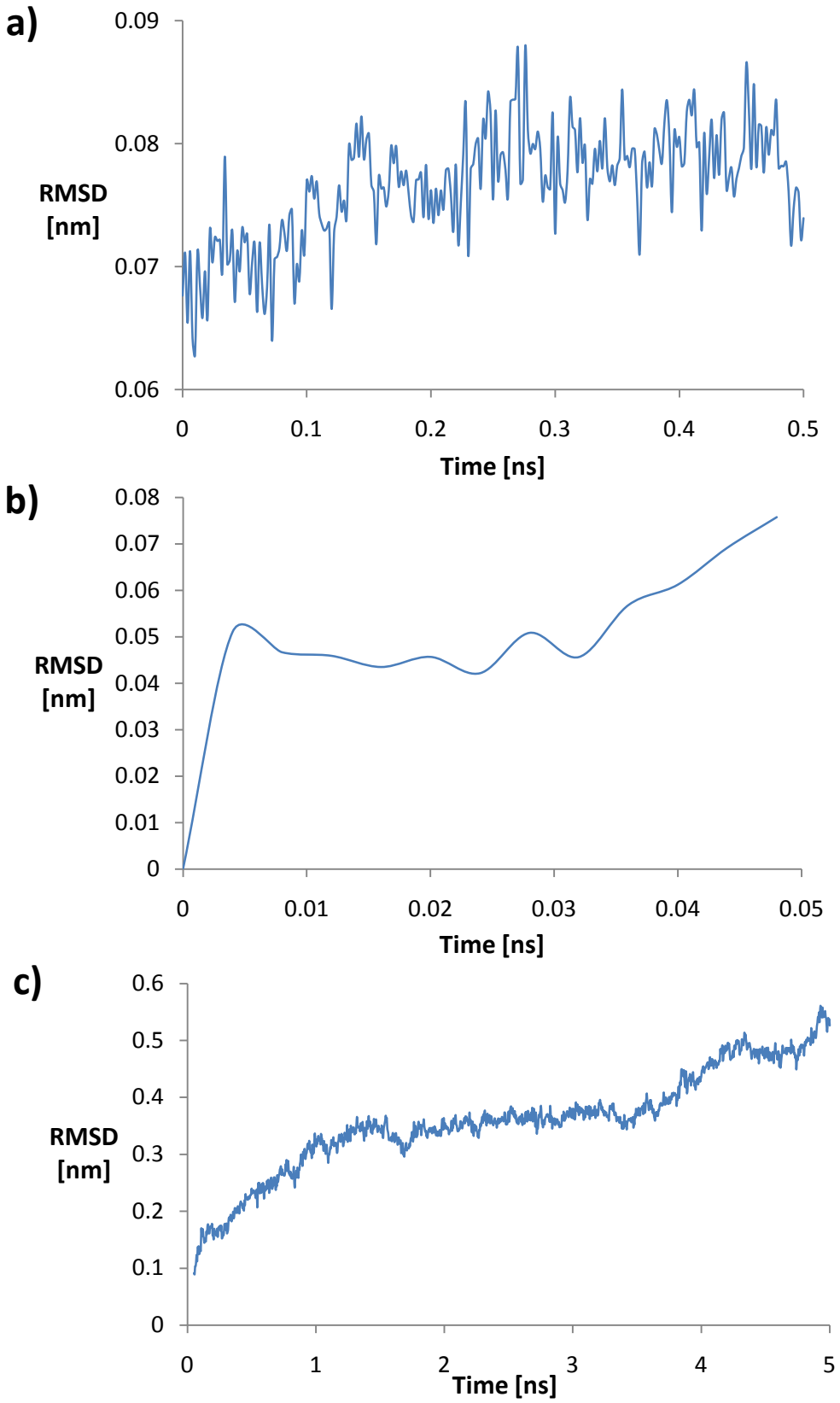

Fig. S8 Plot of root mean square deviation, RMSD, of CAL-B solvated by DCGUA-NO_3 over time during a) the last 500 ps of the 300K MD simulation b) the 50 ps heating phase from 1 to 600K c) the 4.95 ns MD simulation at 600K.

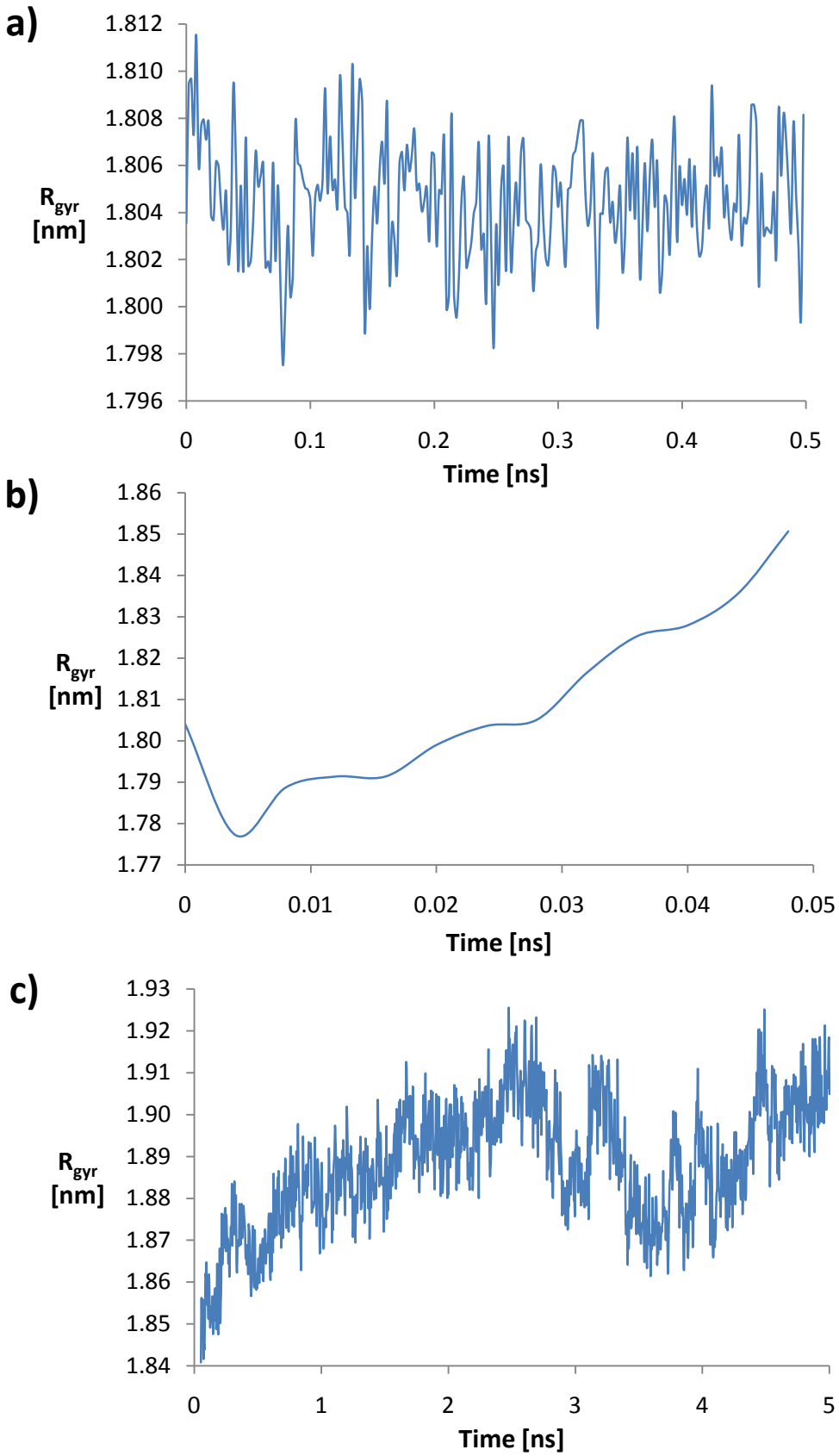

Fig. S9 Plot of radius of gyration, R_{gyr}, of CAL-B solvated by BMIM-PF_6 over time during a) the last 500 ps of the 300K MD simulation b) the 50 ps heating phase from 1 to 600K c) the 4.95 ns MD simulation at 600K.

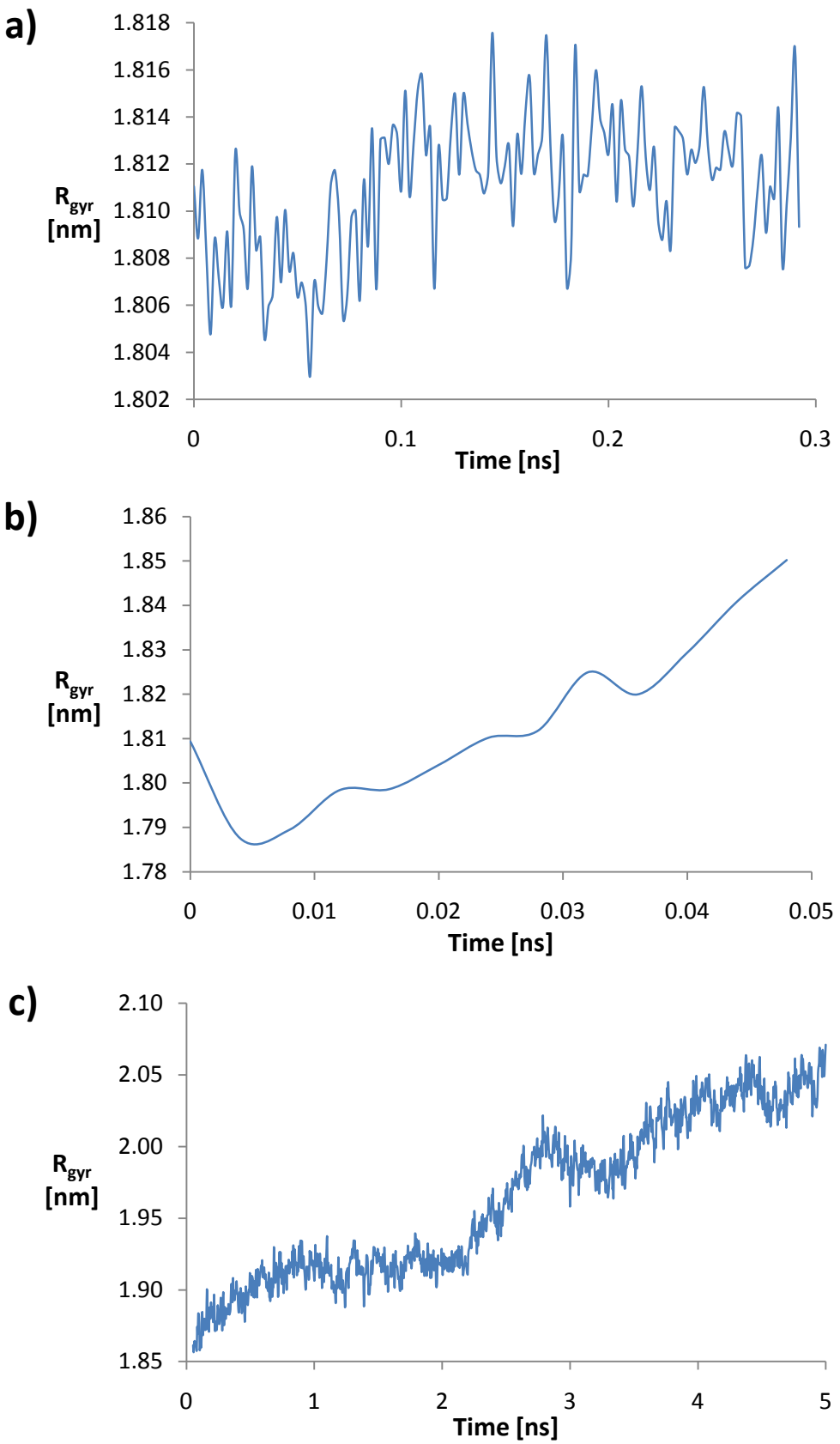

Fig. S10 Plot of radius of gyration, R_{gyr}, of CAL-B solvated by BMIM-NO_3 over time during a) the last 300 ps of the 300K MD simulation b) the 50 ps heating phase from 1 to 600K c) the 4.95 ns MD simulation at 600K.

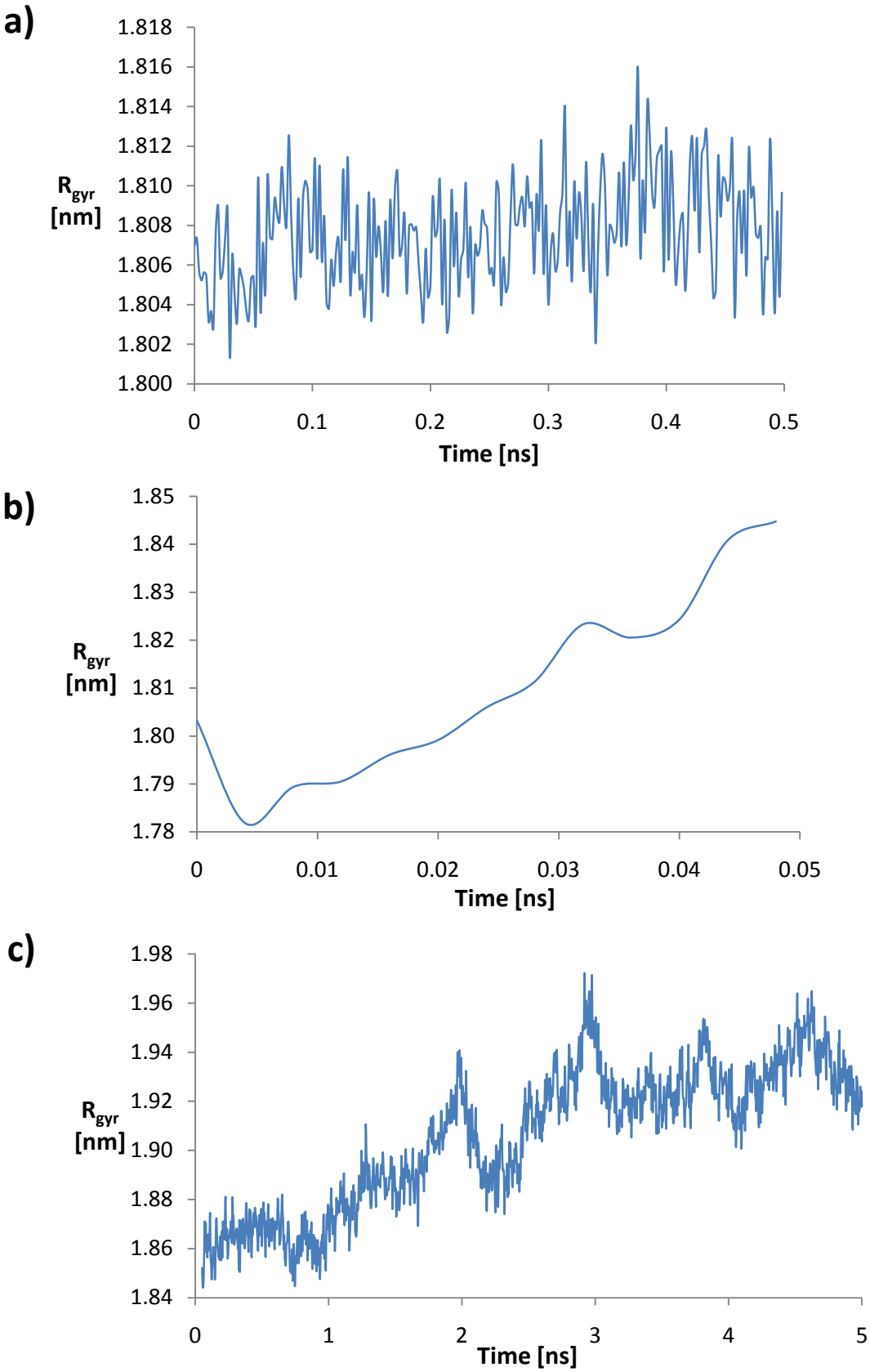

Fig. S11 Plot of radius of gyration, R_{gyr}, of CAL-B solvated by BMIM-BF_4 over time during a) the last 500 ps of the 300K MD simulation b) the 50 ps heating phase from 1 to 600K c) the 4.95 ns MD simulation at 600K.

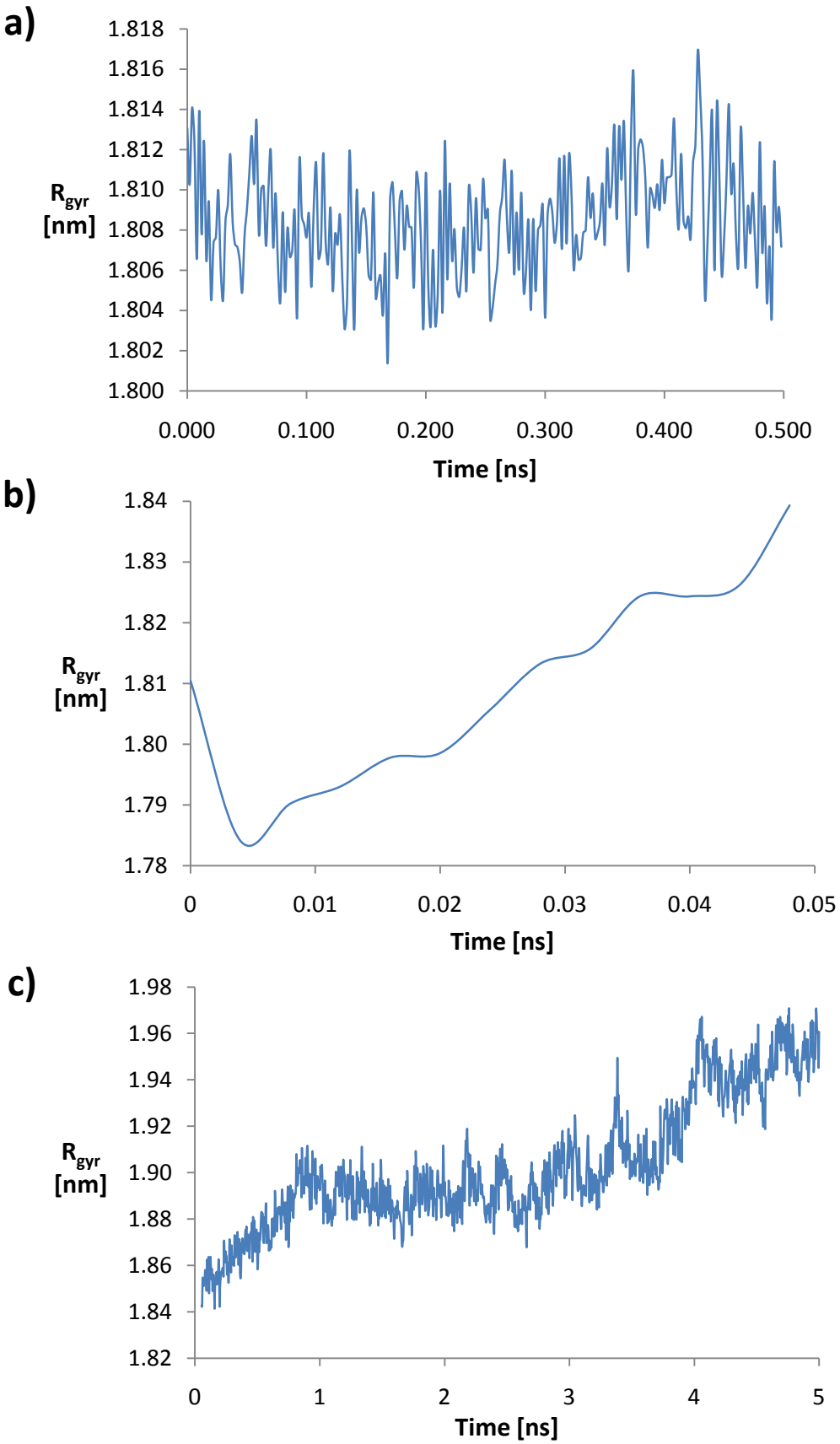

Fig. S12 Plot of radius of gyration, R_{gyr}, of CAL-B solvated by MOEMIM-BF_4 over time during a) the last 500 ps of the 300K MD simulation b) the 50 ps heating phase from 1 to 600K c) the 4.95 ns MD simulation at 600K.

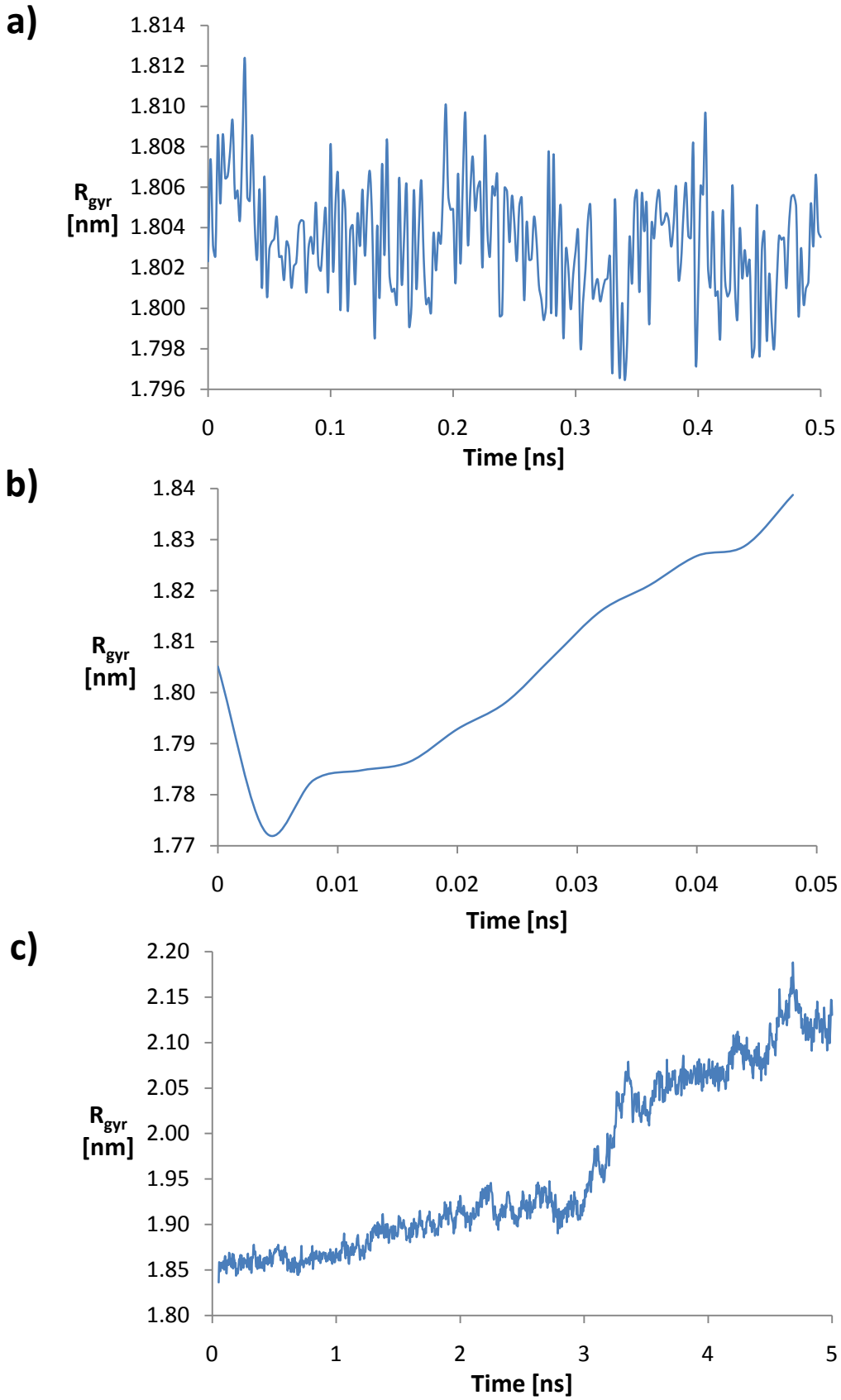

Fig. S13 Plot of radius of gyration, R_{gyr}, of CAL-B solvated by BAGUA-BF_4 over time during a) the last 500 ps of the 300K MD simulation b) the 50 ps heating phase from 1 to 600K c) the 4.95 ns MD simulation at 600K.

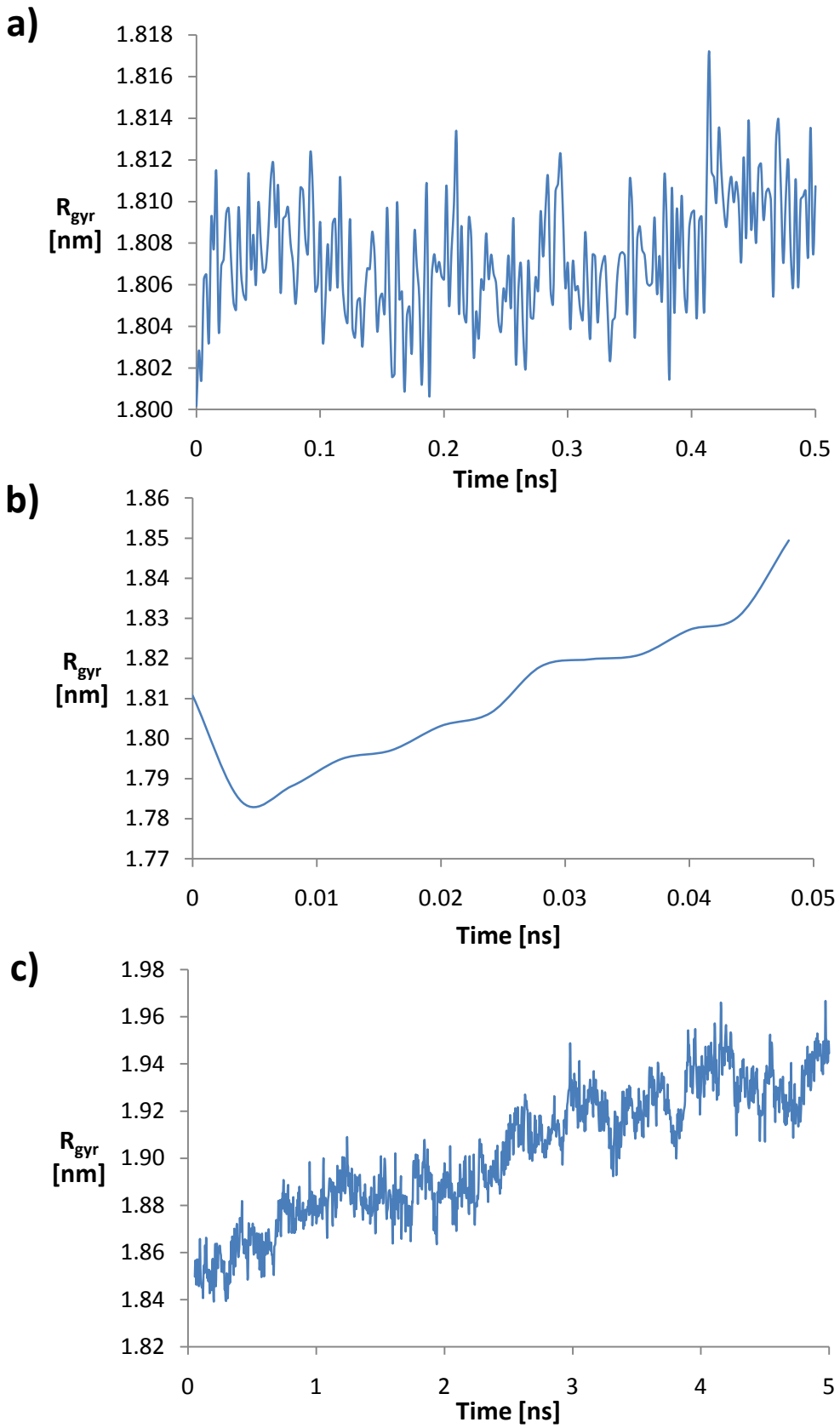

Fig. S14 Plot of radius of gyration, R_{gyr}, of CAL-B solvated by BCGUA-BF_4 over time during a) the last 500 ps of the 300K MD simulation b) the 50 ps heating phase from 1 to 600K c) the 4.95 ns MD simulation at 600K.

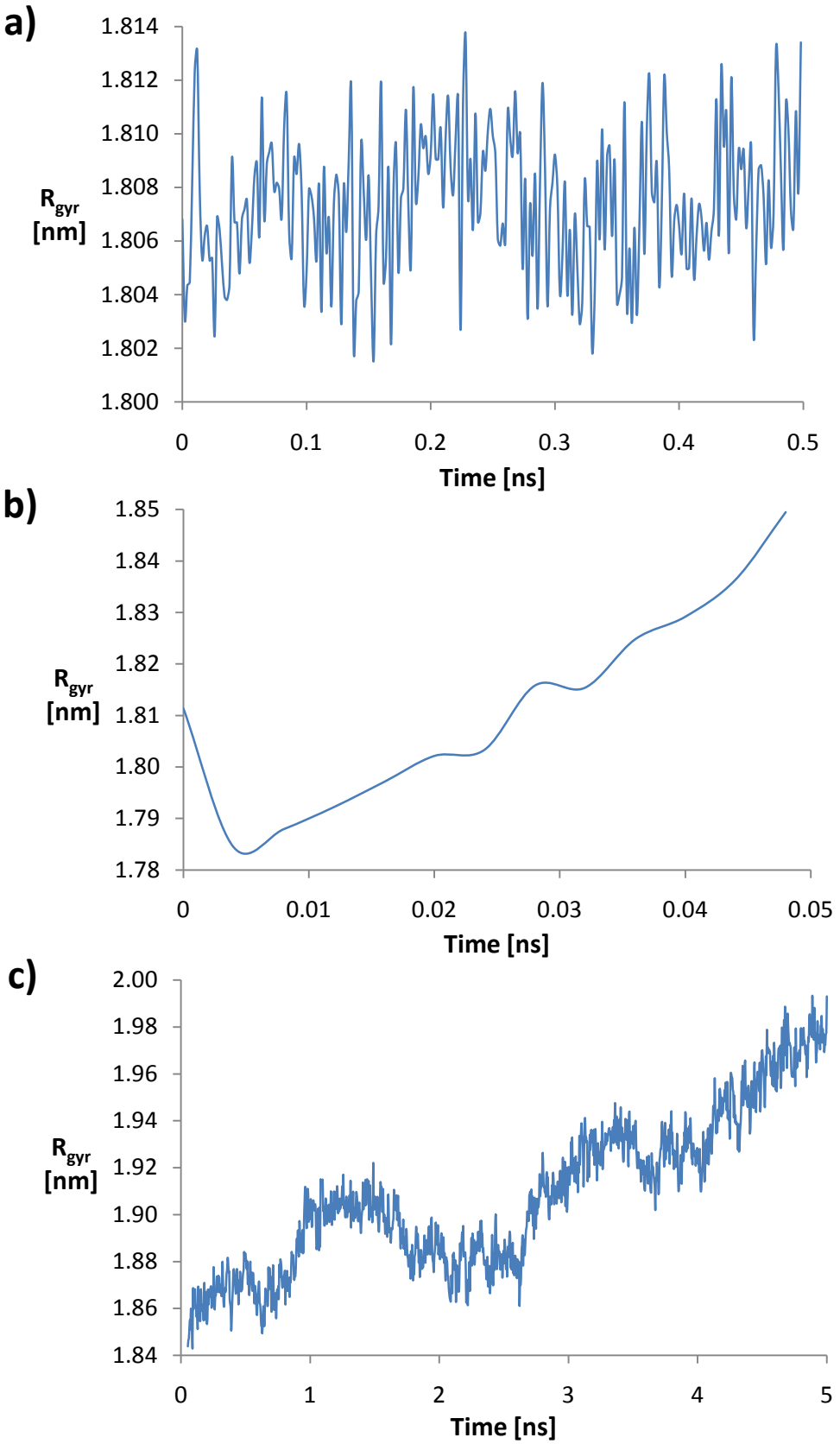

Fig. S15 Plot of radius of gyration, R_{gyr}, of CAL-B solvated by MCGUA-NO_3 over time during a) the last 500 ps of the 300K MD simulation b) the 50 ps heating phase from 1 to 600K c) the 4.95 ns MD simulation at 600K.

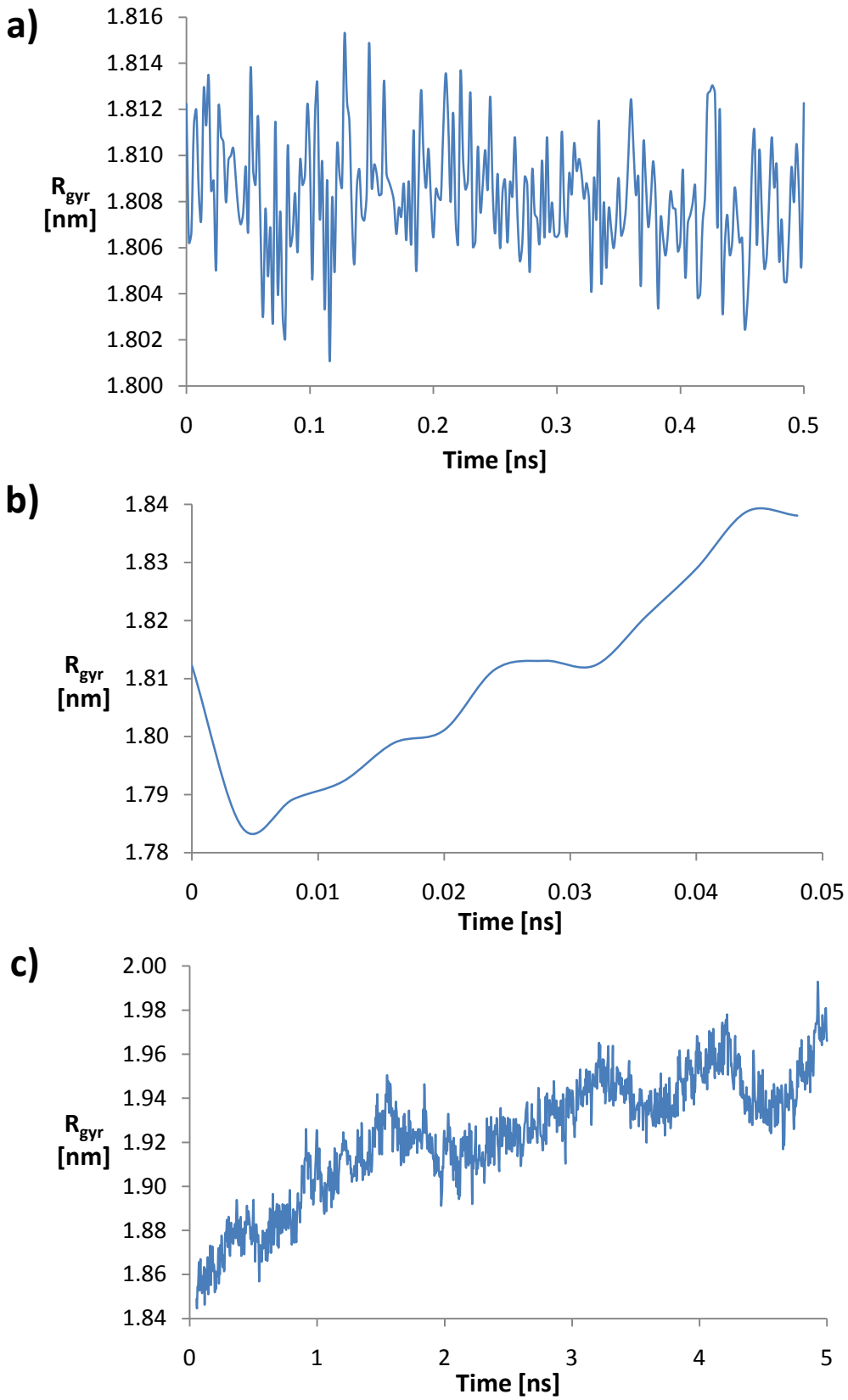

Fig. S16 Plot of radius of gyration, R_{gyr}, of CAL-B solvated by DCGUA-NO_3 over time during a) the last 500 ps of the 300K MD simulation b) the 50 ps heating phase from 1 to 600K c) the 4.95 ns MD simulation at 600K.

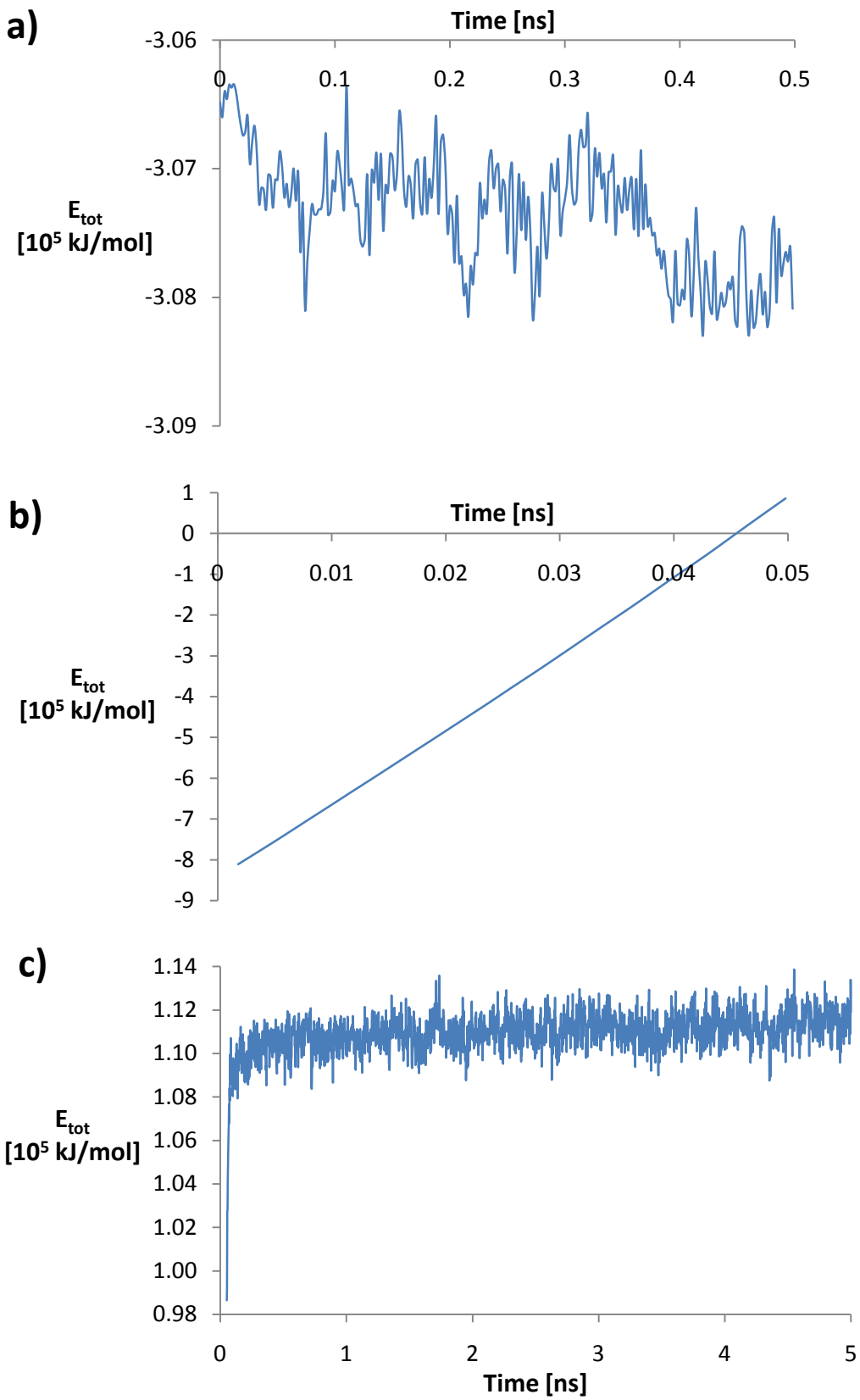

Fig. S17 Plot of total energy, E_{tot}, of CAL-B solvated by BMIM-PF_6 over time during a) the last 500 ps of the 300K MD simulation b) the 50 ps heating phase from 1 to 600K c) the 4.95 ns MD simulation at 600K.

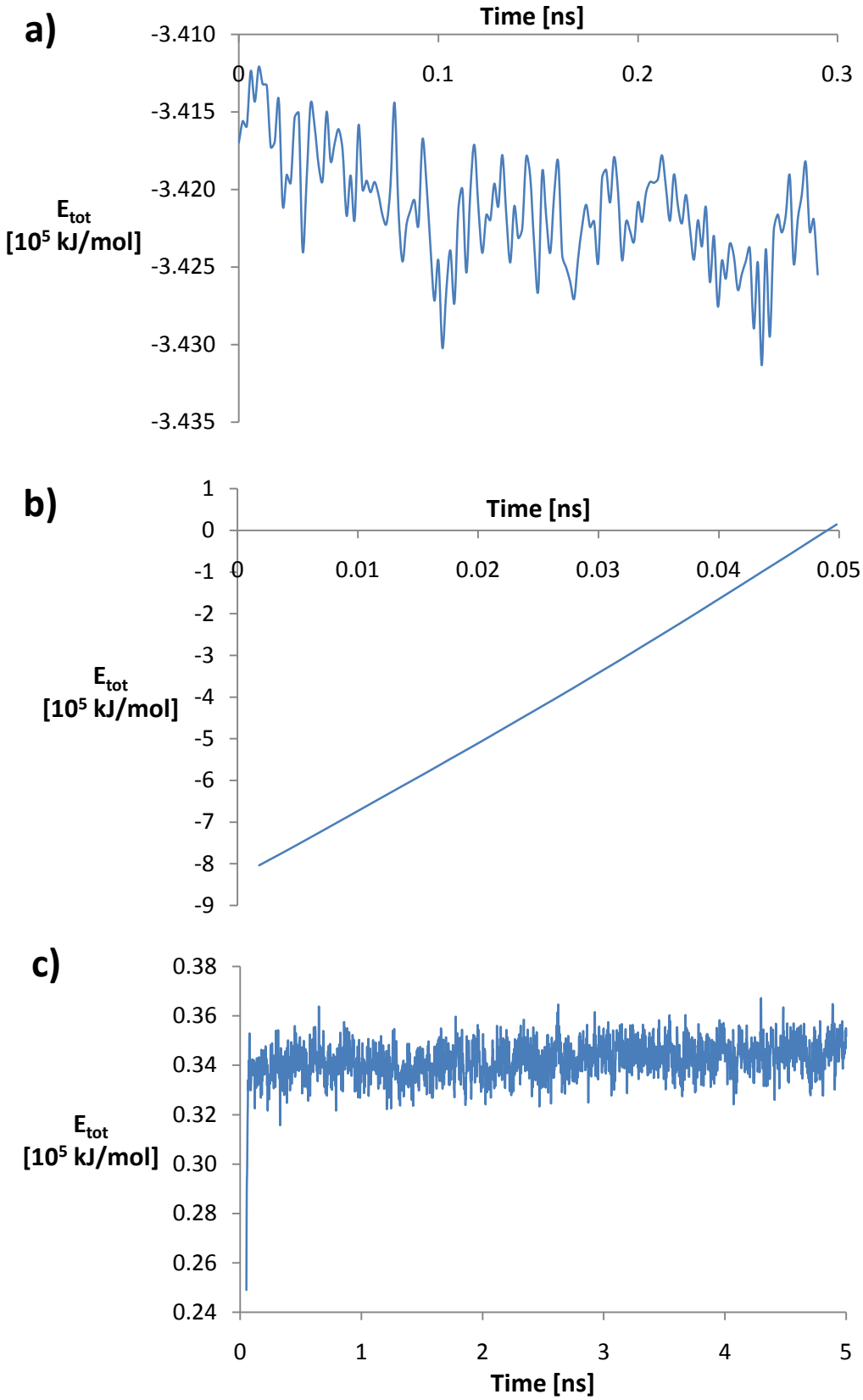

Fig. S18 Plot of total energy, E_{tot}, of CAL-B solvated by BMIM-NO_3 over time during a) the last 300 ps of the 300K MD simulation b) the 50 ps heating phase from 1 to 600K c) the 4.95 ns MD simulation at 600K.

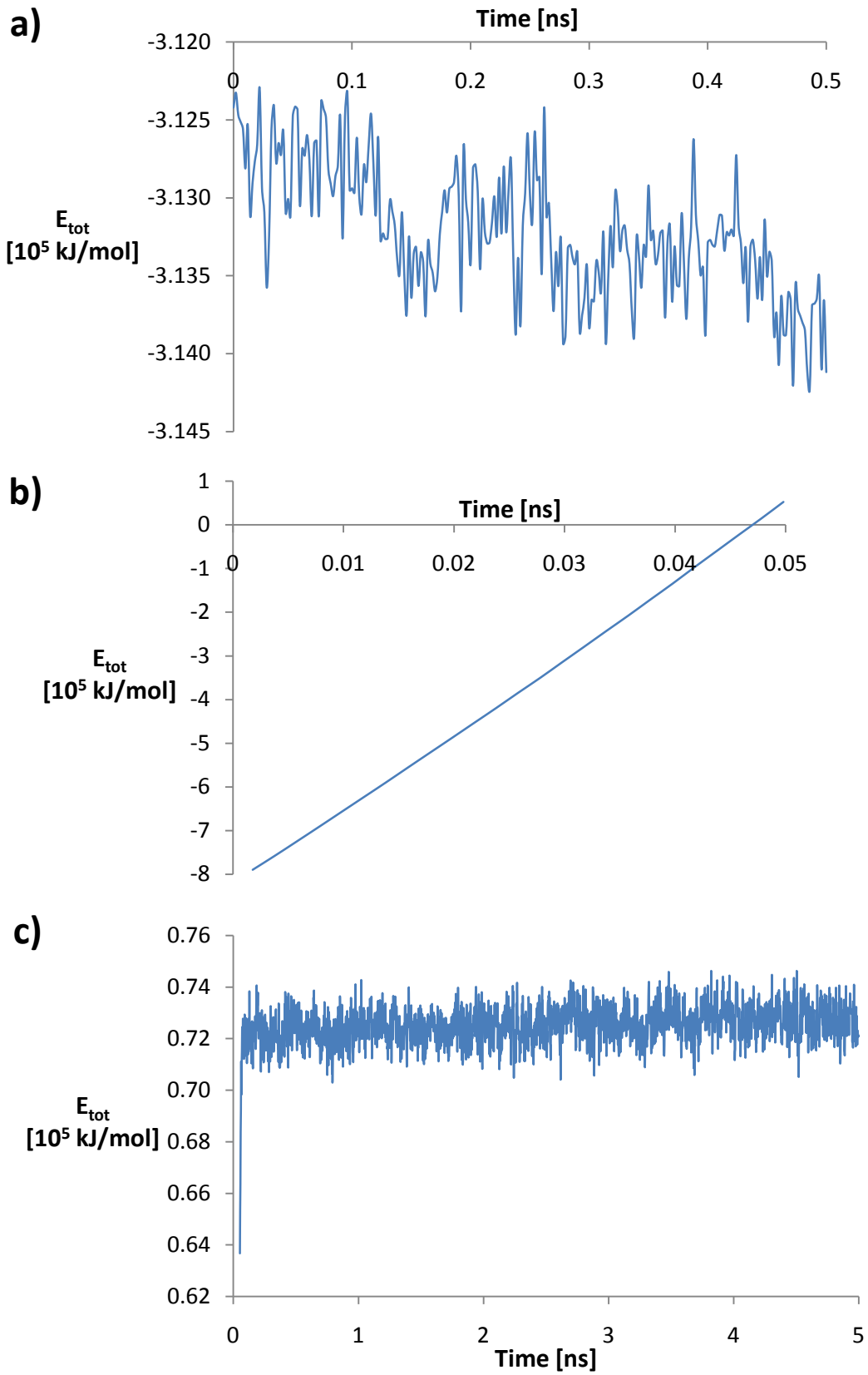

Fig. S19 Plot of total energy, E_{tot}, of CAL-B solvated by BMIM-BF_4 over time during a) the last 500 ps of the 300K MD simulation b) the 50 ps heating phase from 1 to 600K c) the 4.95 ns MD simulation at 600K.

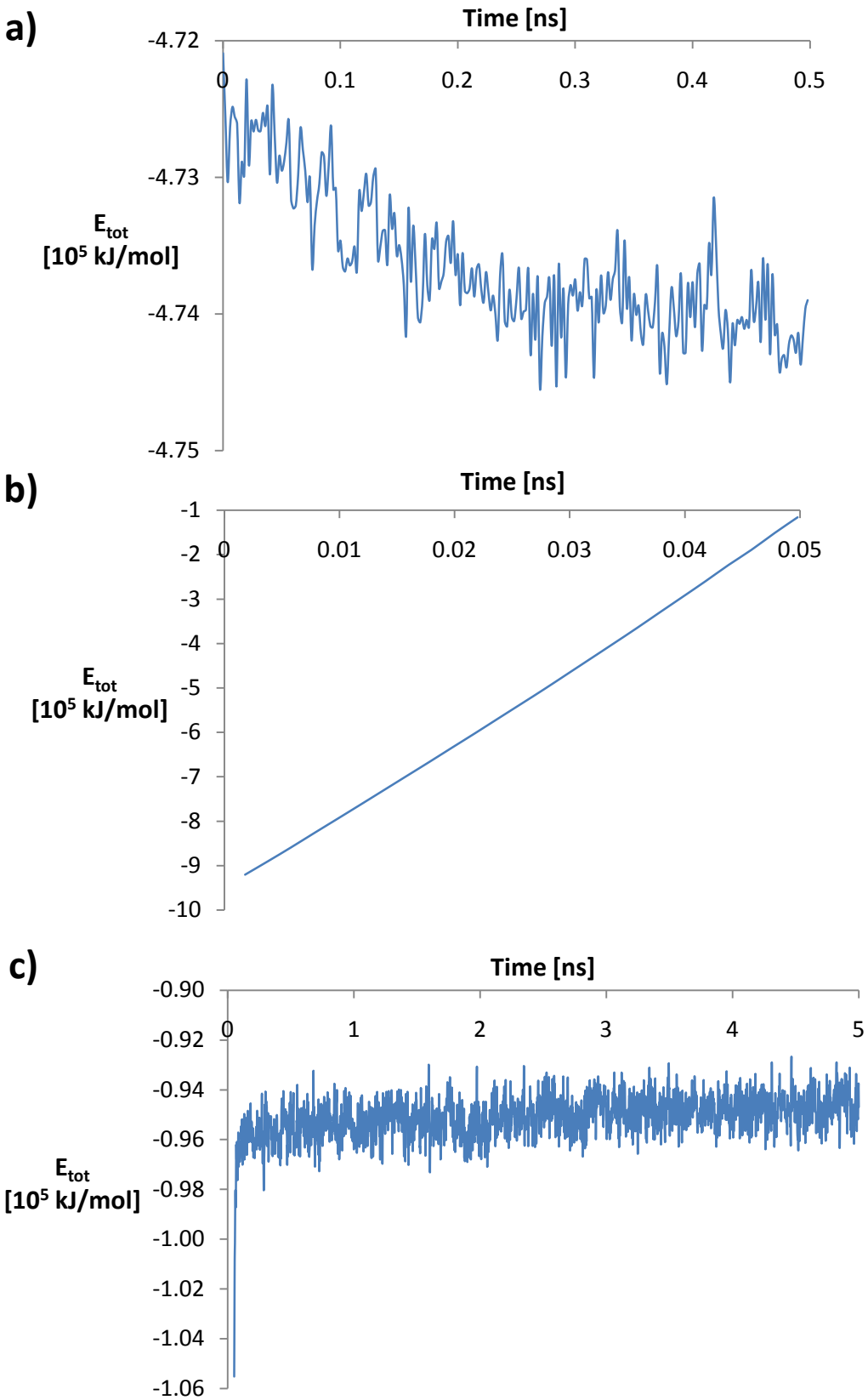

Fig. S20 Plot of total energy, E_{tot}, of CAL-B solvated by MOEMIM-BF_4 over time during a) the last 500 ps of the 300K MD simulation b) the 50 ps heating phase from 1 to 600K c) the 4.95 ns MD simulation at 600K.

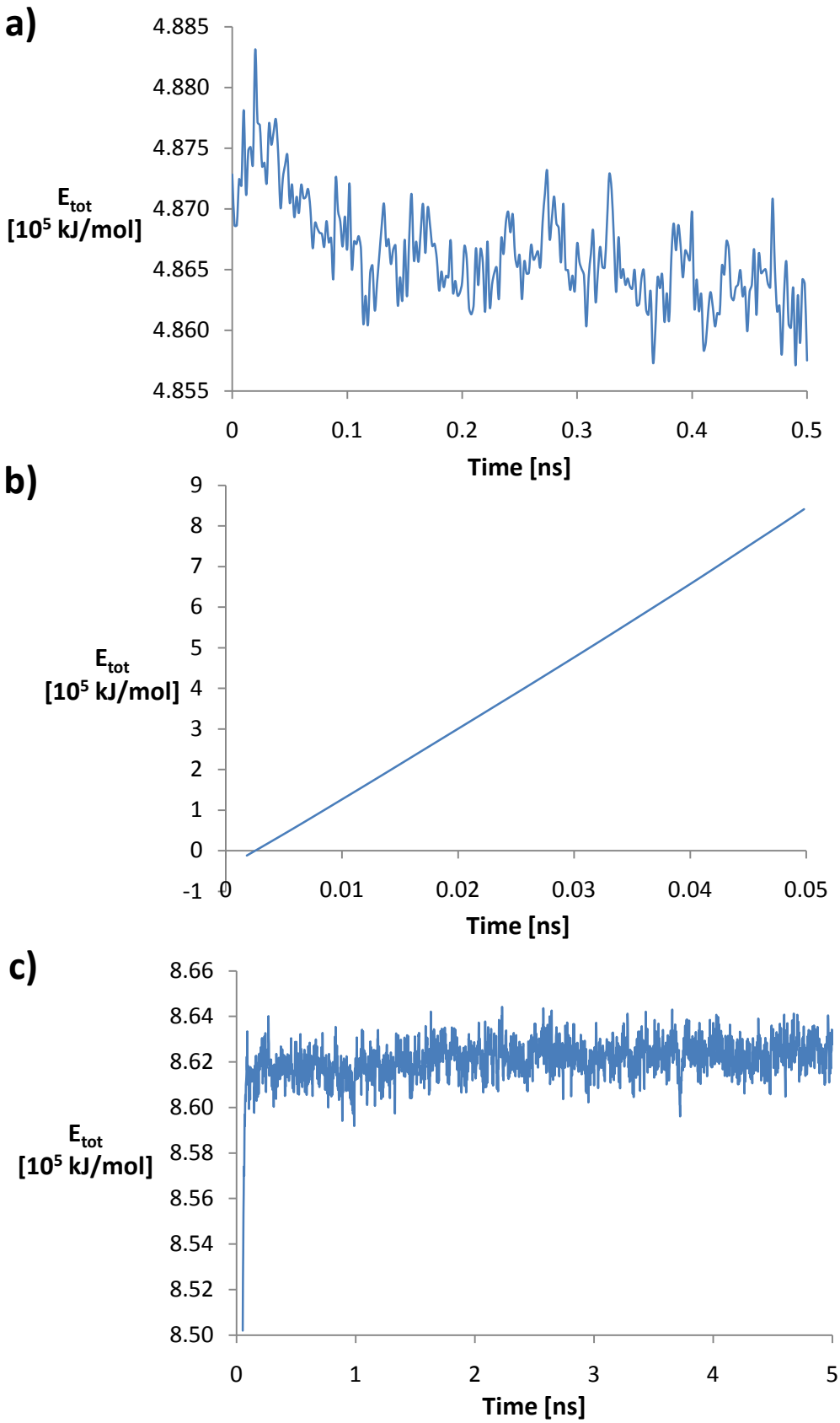

Fig. S21 Plot of total energy, E_{tot}, of CAL-B solvated by BAGUA-BF_4 over time during a) the last 500 ps of the 300K MD simulation b) the 50 ps heating phase from 1 to 600K c) the 4.95 ns MD simulation at 600K.

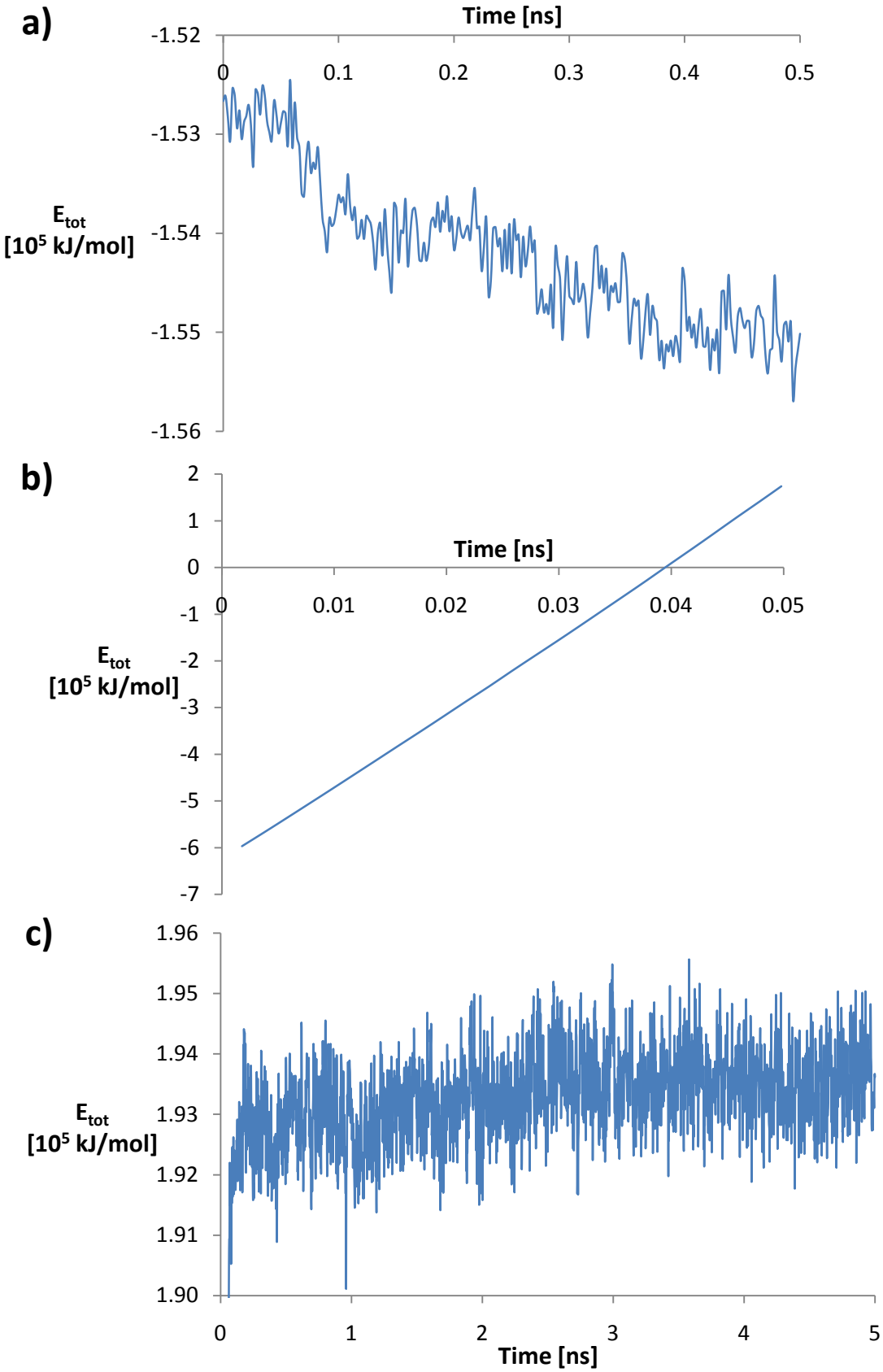

Fig. S22 Plot of total energy, E_{tot}, of CAL-B solvated by BCGUA-BF_4 over time during a) the last 500 ps of the 300K MD simulation b) the 50 ps heating phase from 1 to 600K c) the 4.95 ns MD simulation at 600K.

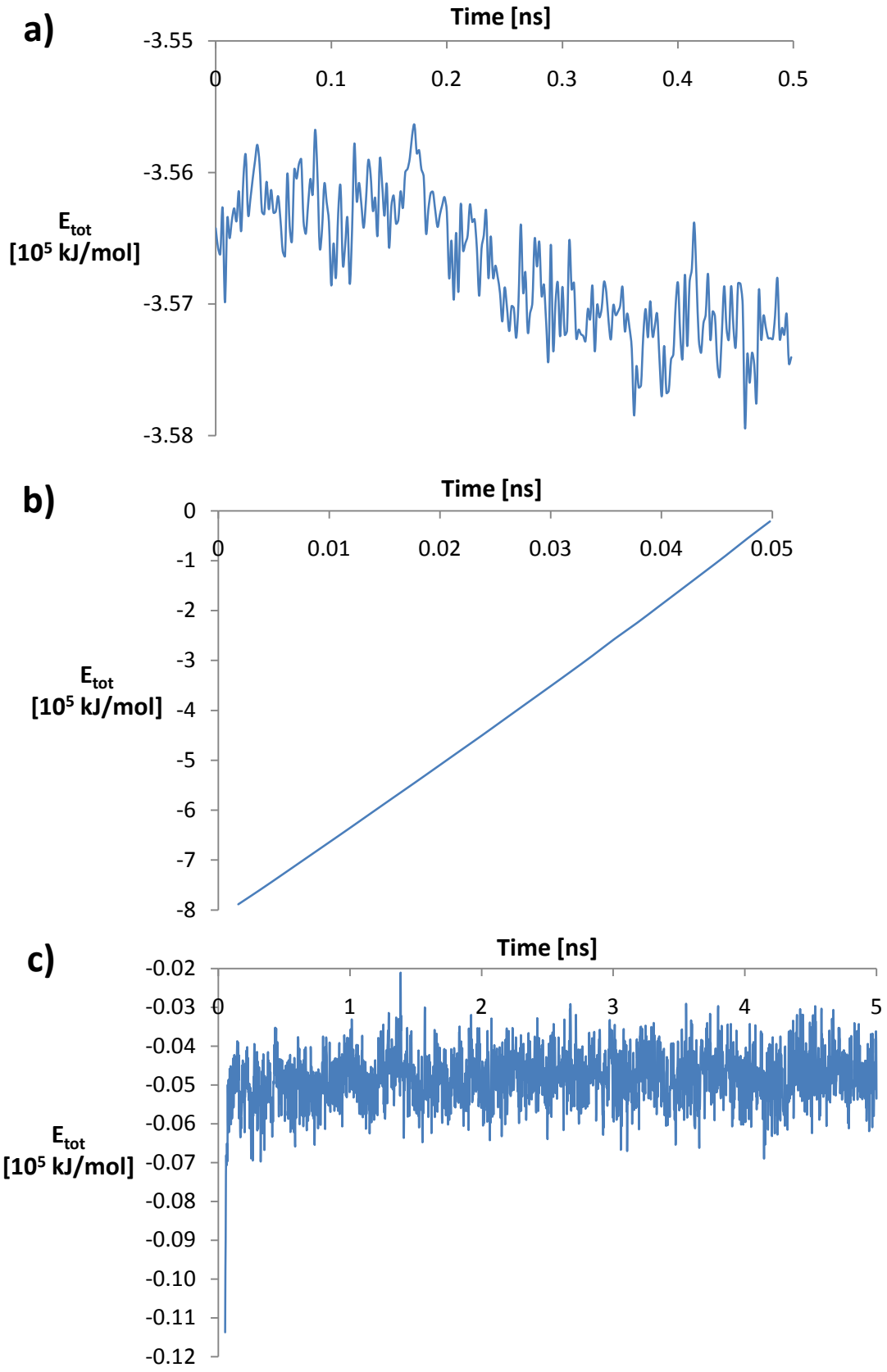

Fig. S23 Plot of total energy, E_{tot}, of CAL-B solvated by MCGUA-NO_3 over time during a) the last 500 ps of the 300K MD simulation b) the 50 ps heating phase from 1 to 600K c) the 4.95 ns MD simulation at 600K.

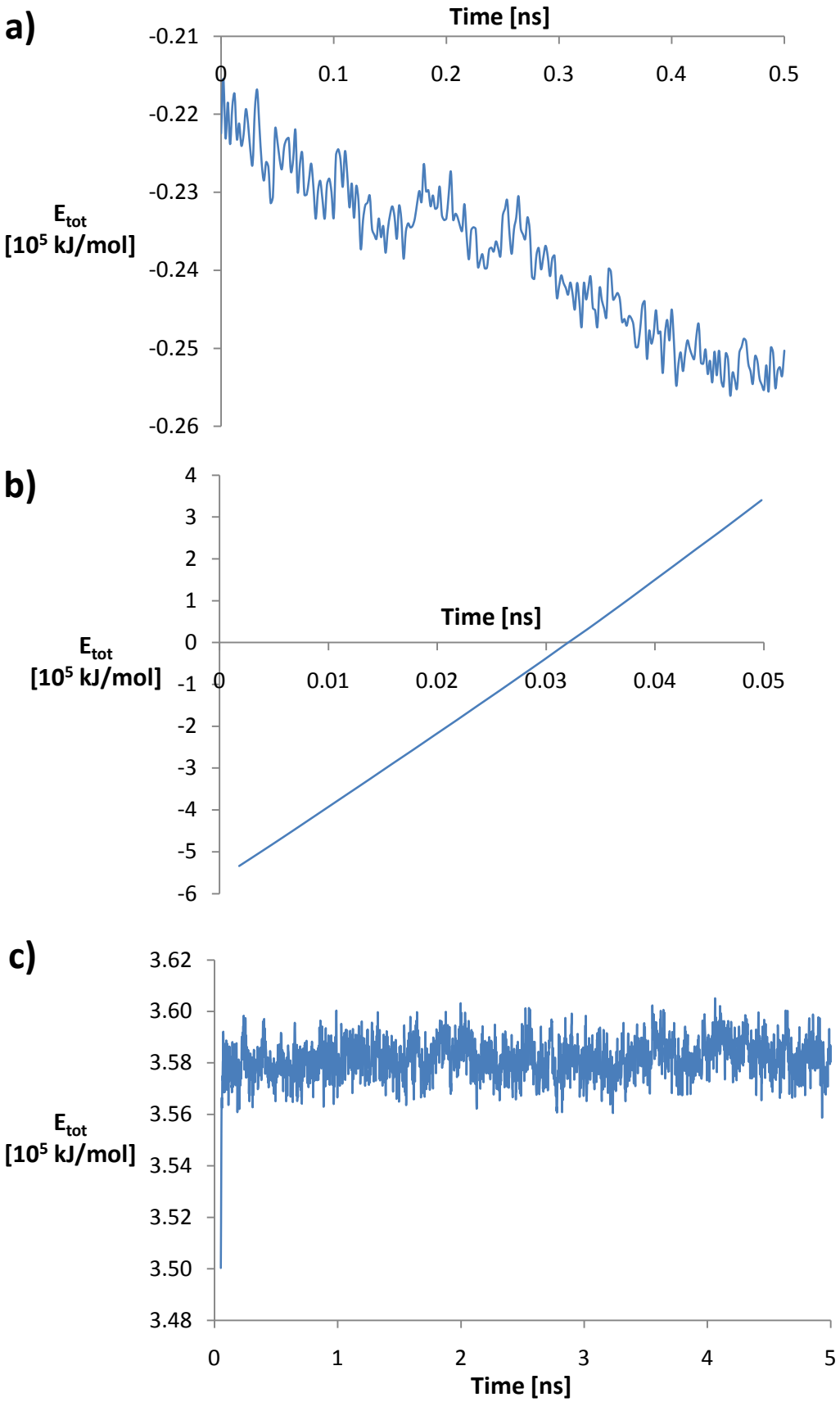

Fig. S24 Plot of total energy, E_{tot}, of CAL-B solvated by DCGUA-NO_3 over time during a) the last 500 ps of the 300K MD simulation b) the 50 ps heating phase from 1 to 600K c) the 4.95 ns MD simulation at 600K.

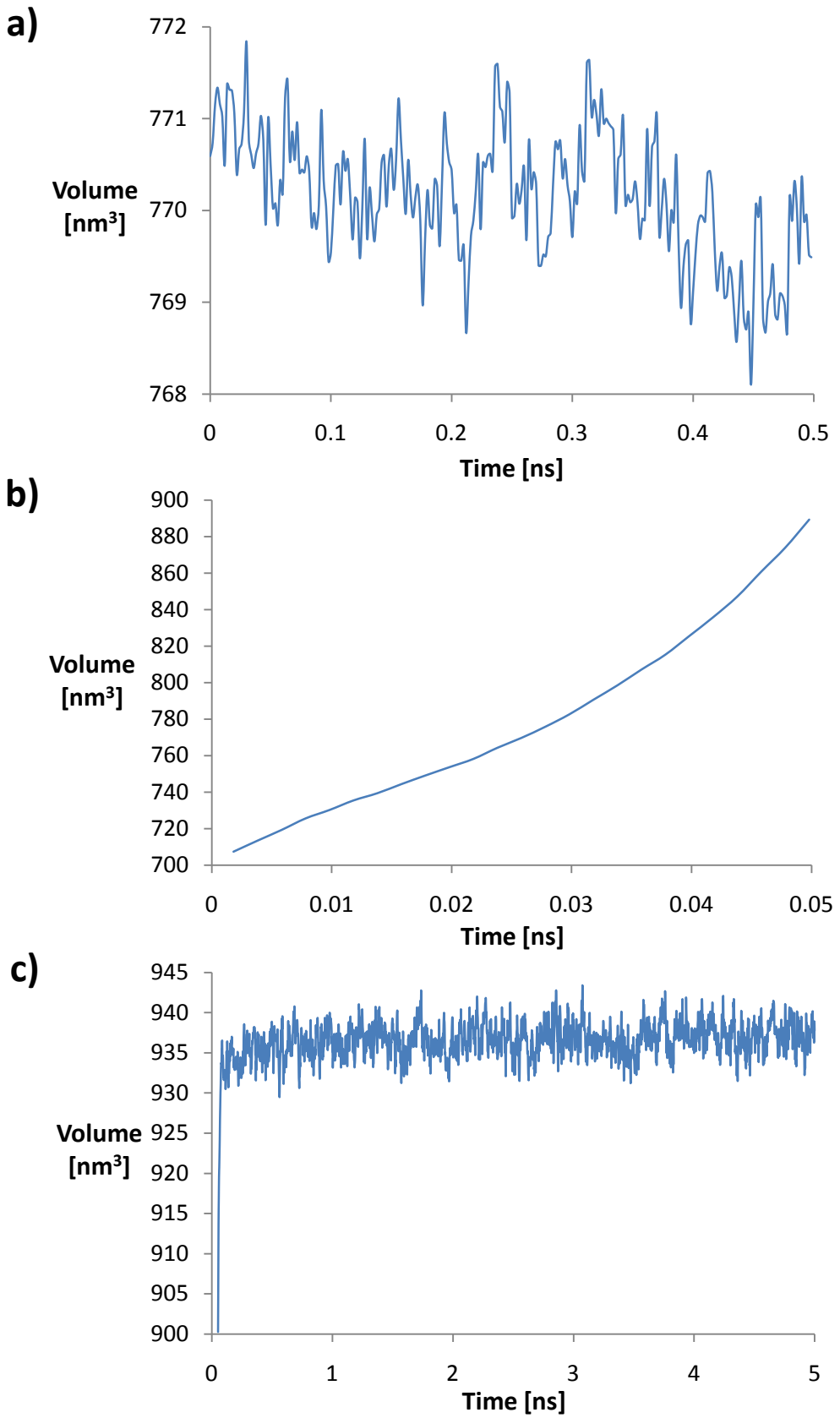

Fig. S25 Plot of box volume containing CAL-B solvated by BMIM-PF_6 over time during a) the last 500 ps of the 300K MD simulation b) the 50 ps heating phase from 1 to 600K c) the 4.95 ns MD simulation at 600K.

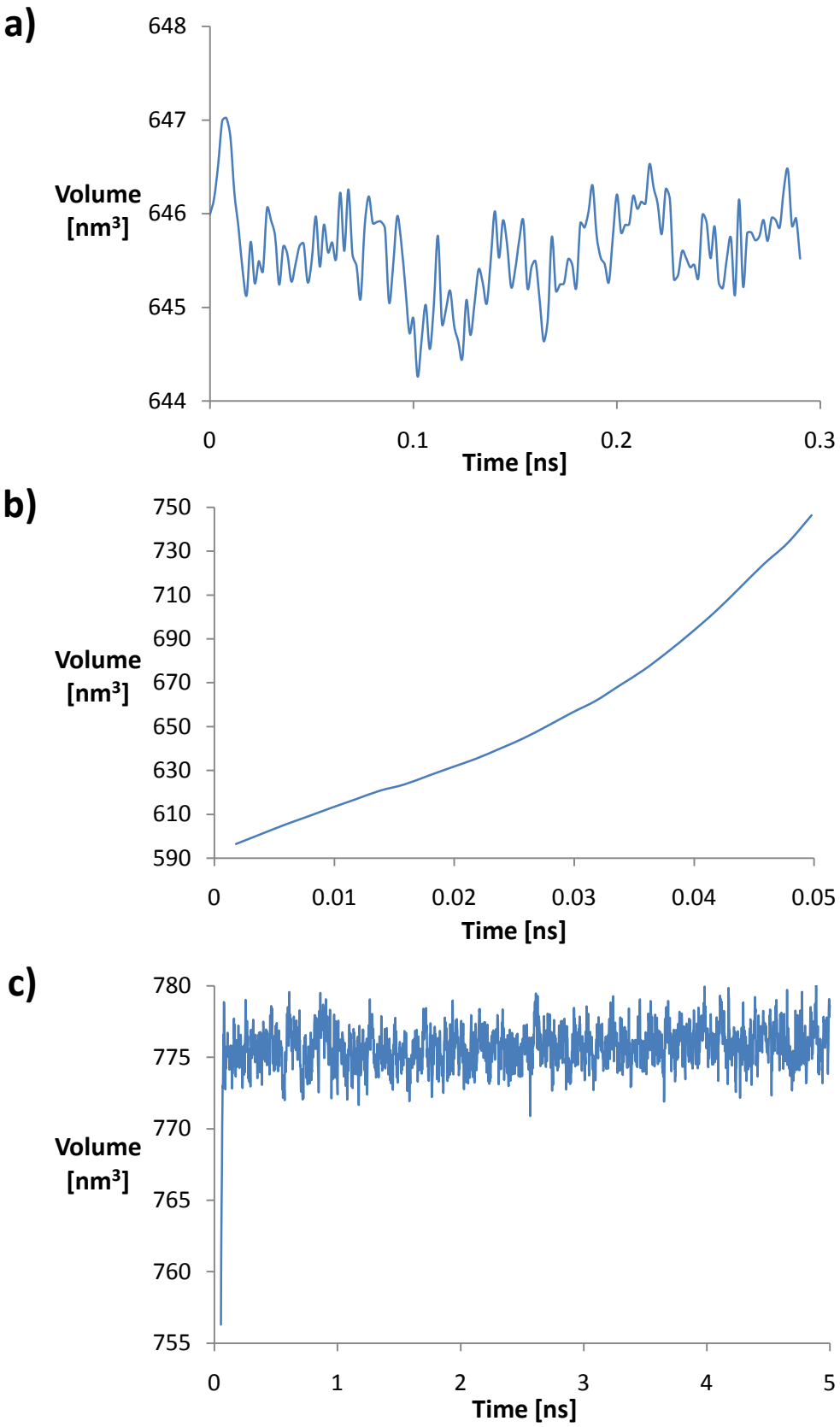

Fig. S26 Plot of box volume containing CAL-B solvated by BMIM-NO_3 over time during a) the last 300 ps of the 300K MD simulation b) the 50 ps heating phase from 1 to 600K c) the 4.95 ns MD simulation at 600K.

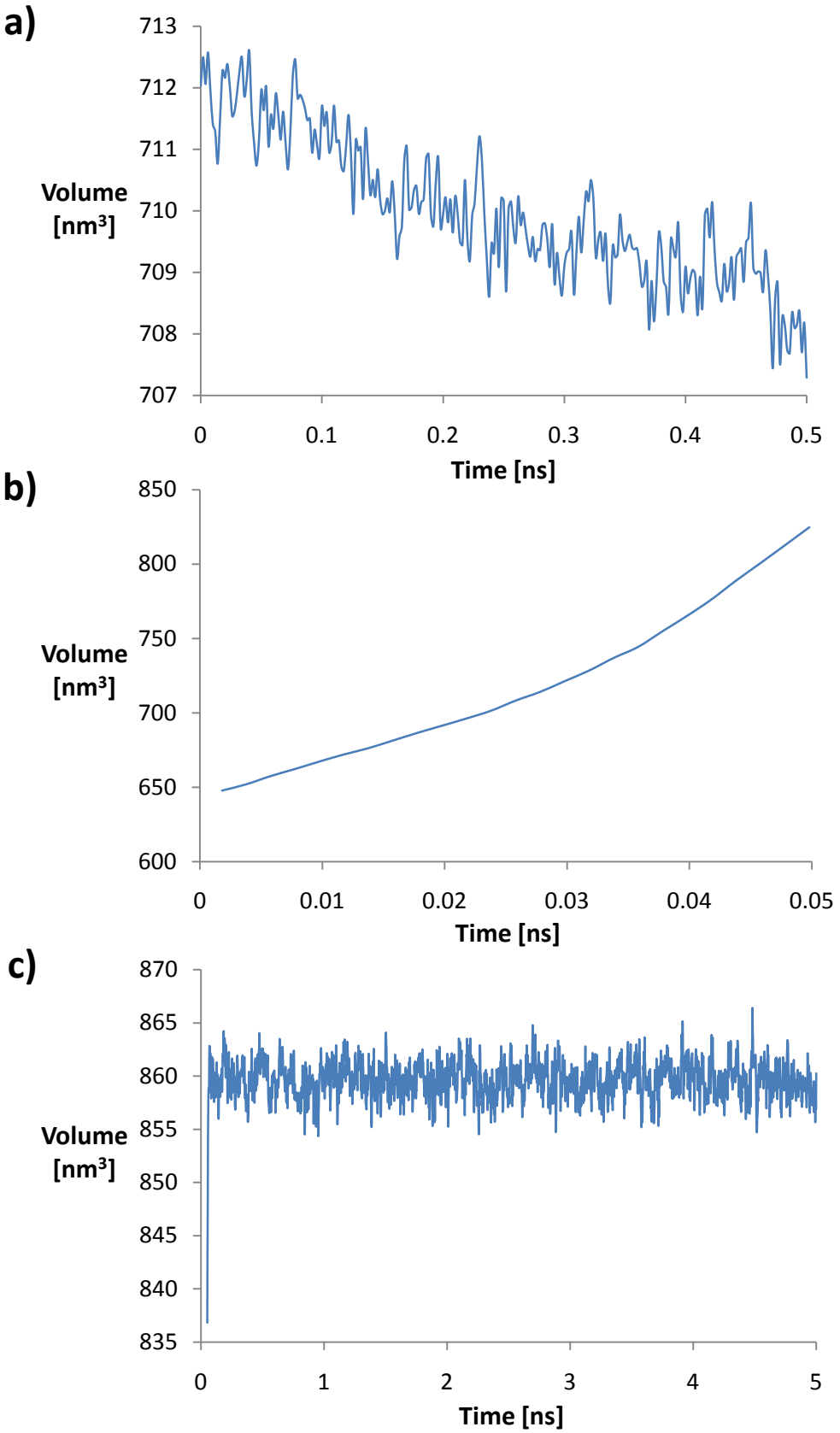

Fig. S27 Plot of box volume containing CAL-B solvated by BMIM-BF_4 over time during a) the last 500 ps of the 300K MD simulation b) the 50 ps heating phase from 1 to 600K c) the 4.95 ns MD simulation at 600K.

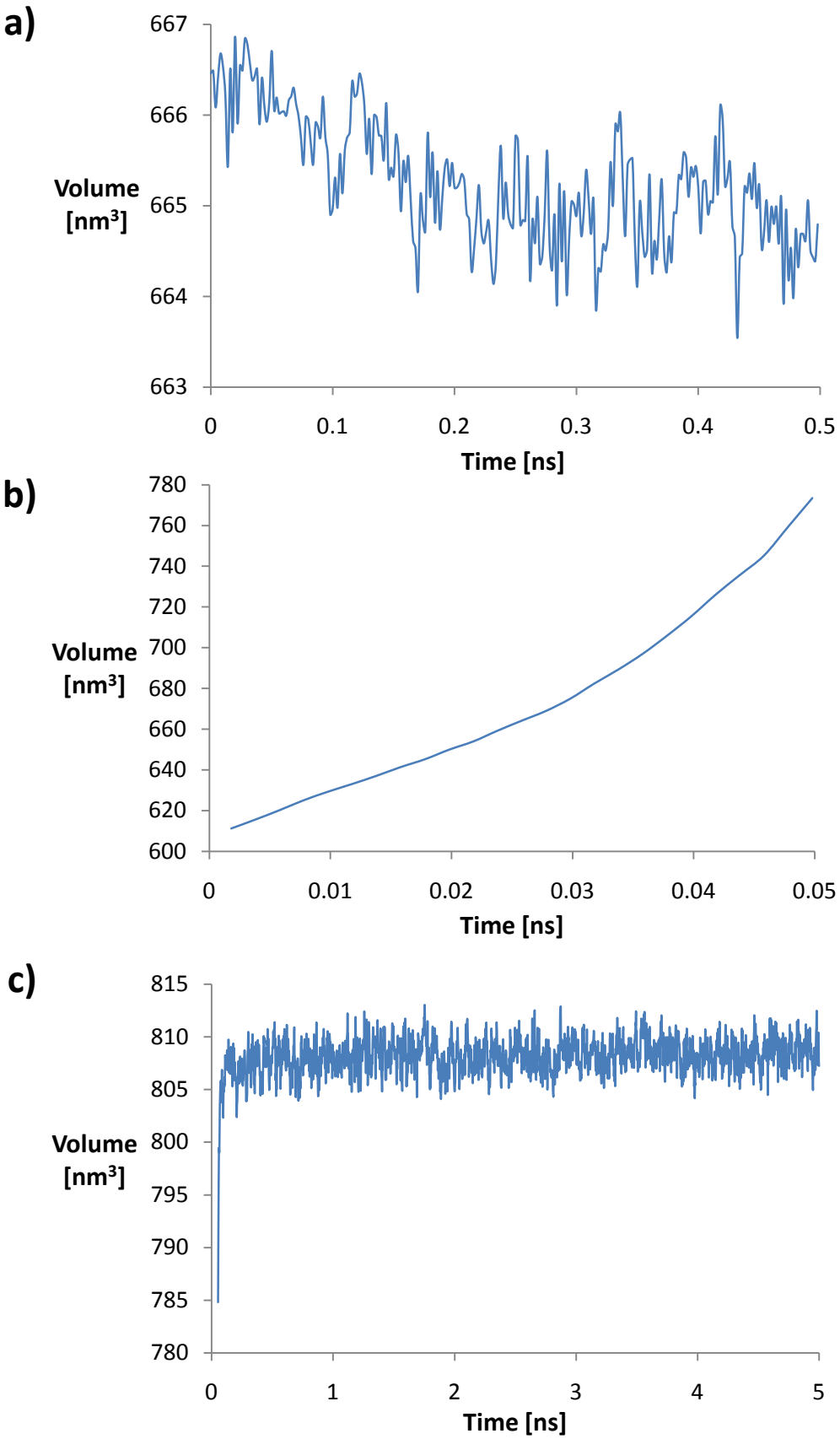

Fig. S28 Plot of box volume containing CAL-B solvated by MOEMIM-BF_4 over time during a) the last 500 ps of the 300K MD simulation b) the 50 ps heating phase from 1 to 600K c) the 4.95 ns MD simulation at 600K.

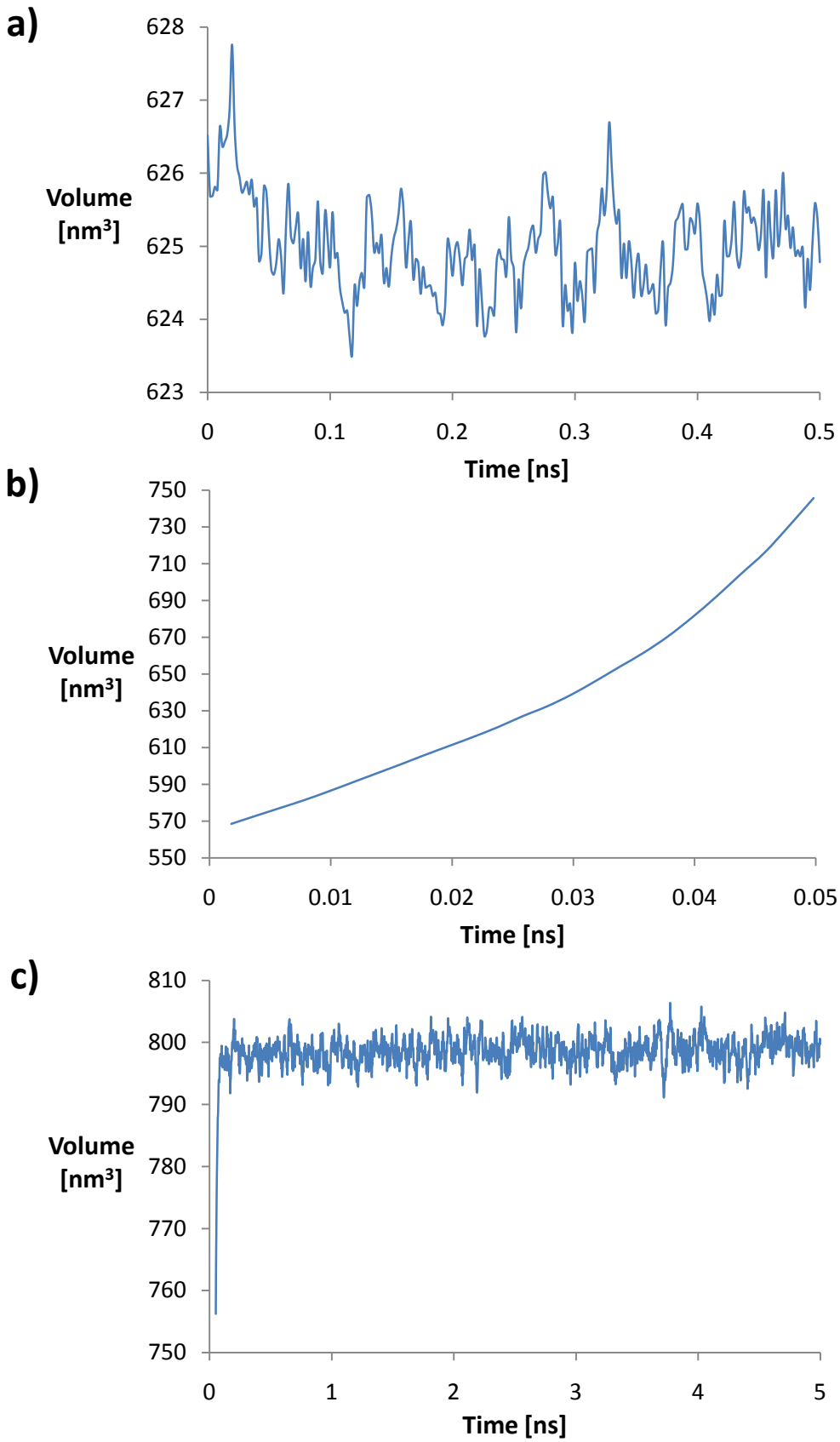

Fig. S29 Plot of box volume containing CAL-B solvated by BAGUA-BF_4 over time during a) the last 500 ps of the 300K MD simulation b) the 50 ps heating phase from 1 to 600K c) the 4.95 ns MD simulation at 600K.

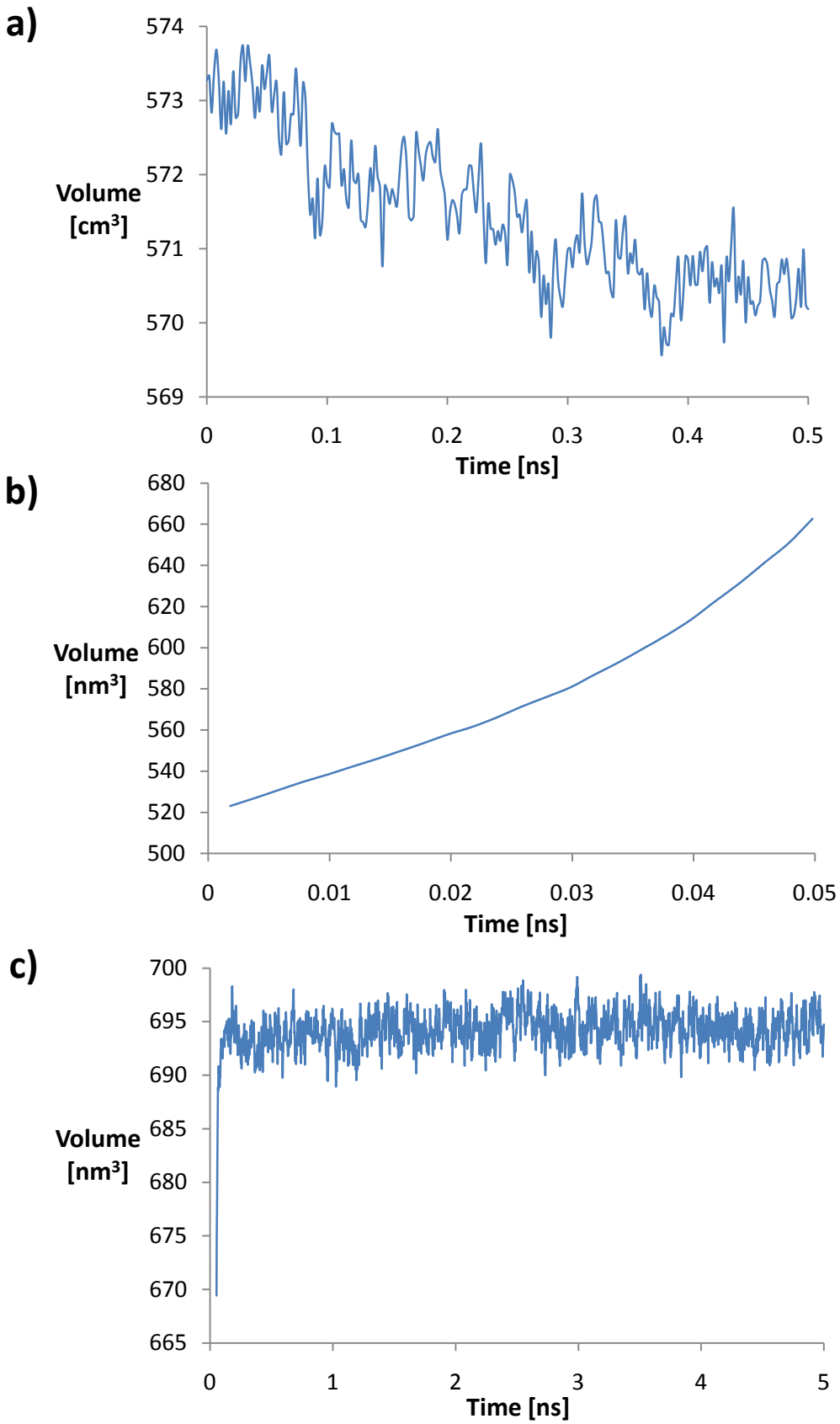

Fig. S30 Plot of box volume containing CAL-B solvated by BCGUA-BF_4 over time during a) the last 500 ps of the 300K MD simulation b) the 50 ps heating phase from 1 to 600K c) the 4.95 ns MD simulation at 600K.

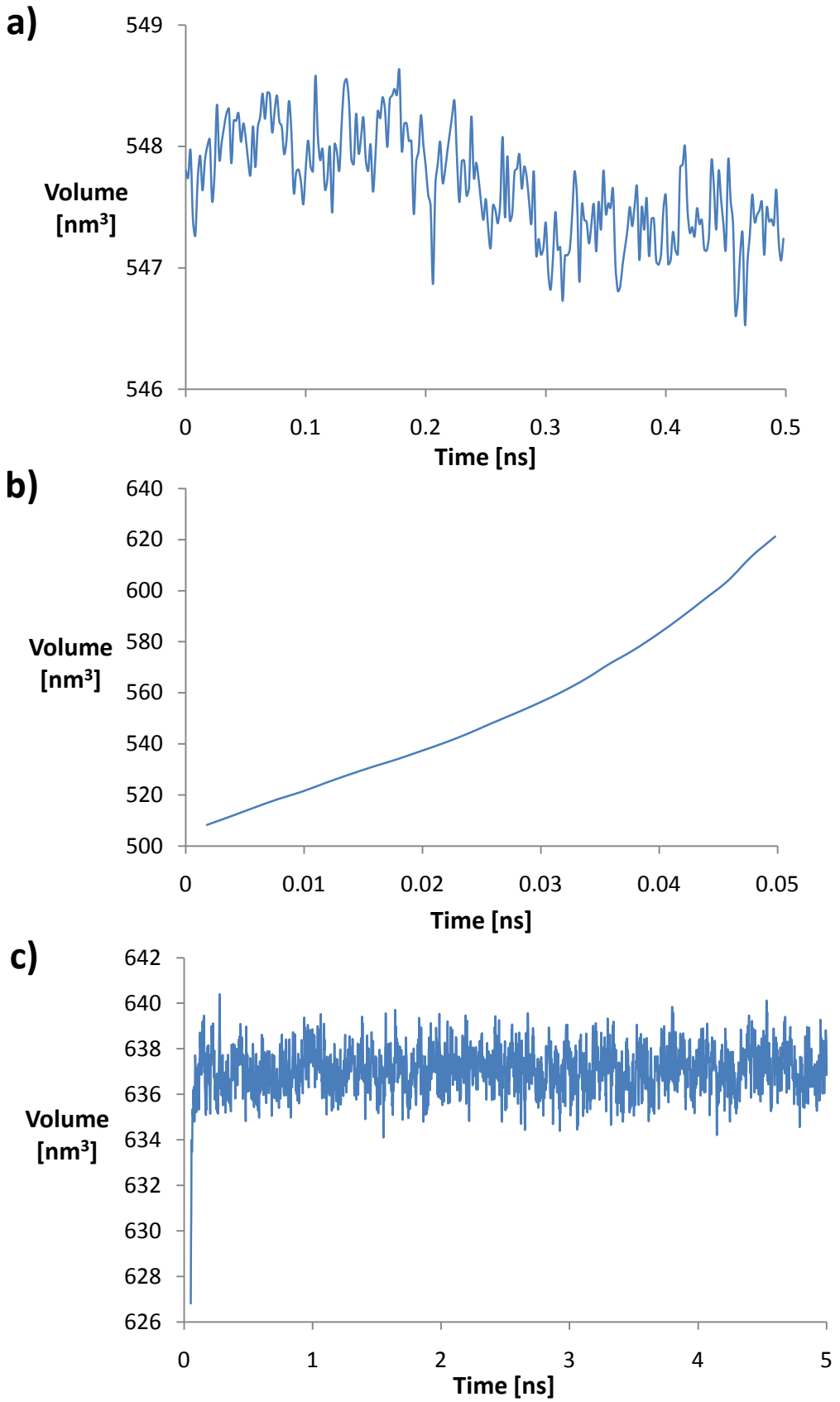

Fig. S31 Plot of box volume containing CAL-B solvated by MCGUA-NO_3 over time during a) the last 500 ps of the 300K MD simulation b) the 50 ps heating phase from 1 to 600K c) the 4.95 ns MD simulation at 600K.

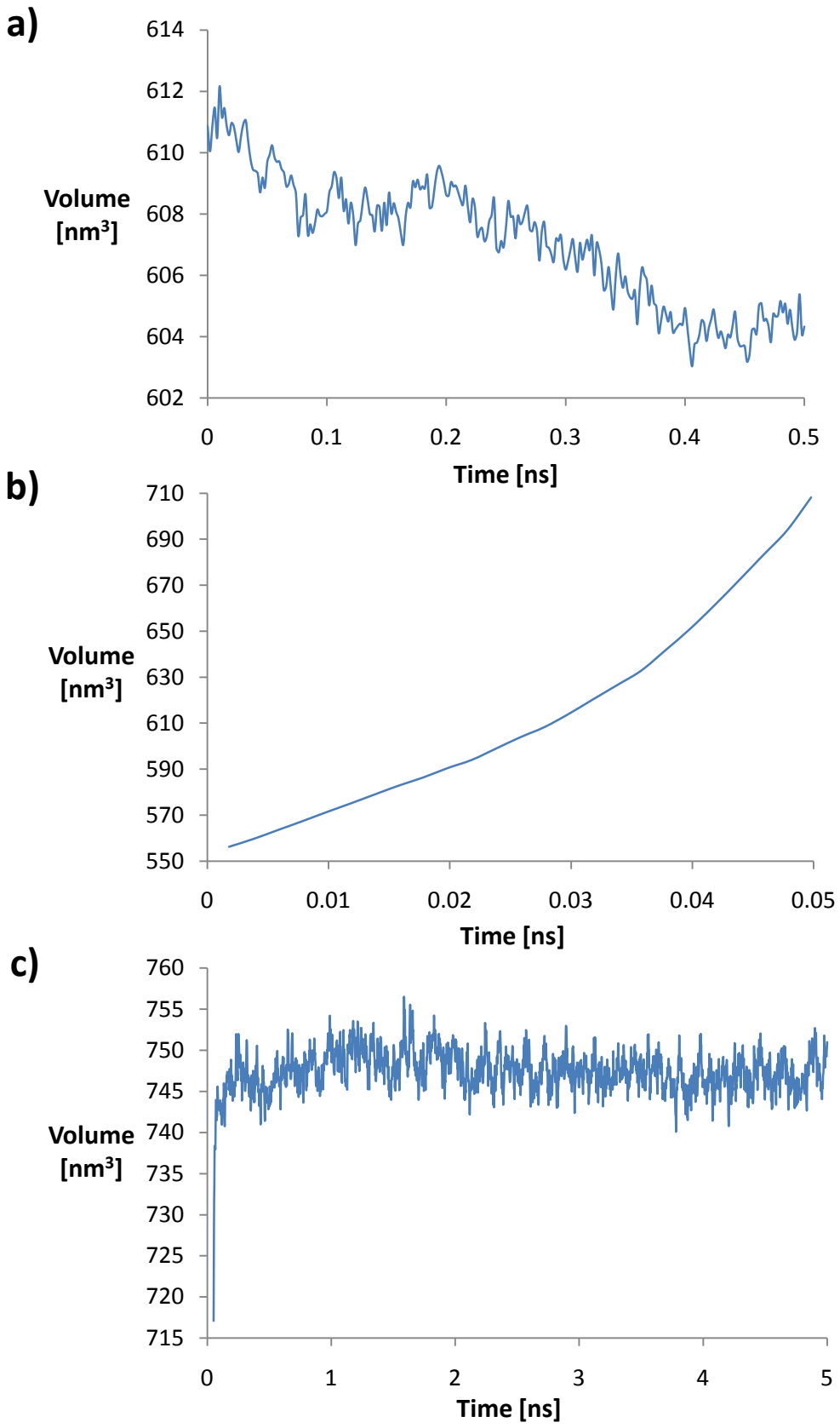

Fig. S32 Plot of box volume containing CAL-B solvated by DCGUA-NO_3 over time during a) the last 500 ps of the 300K MD simulation b) the 50 ps heating phase from 1 to 600K c) the 4.95 ns MD simulation at 600K.

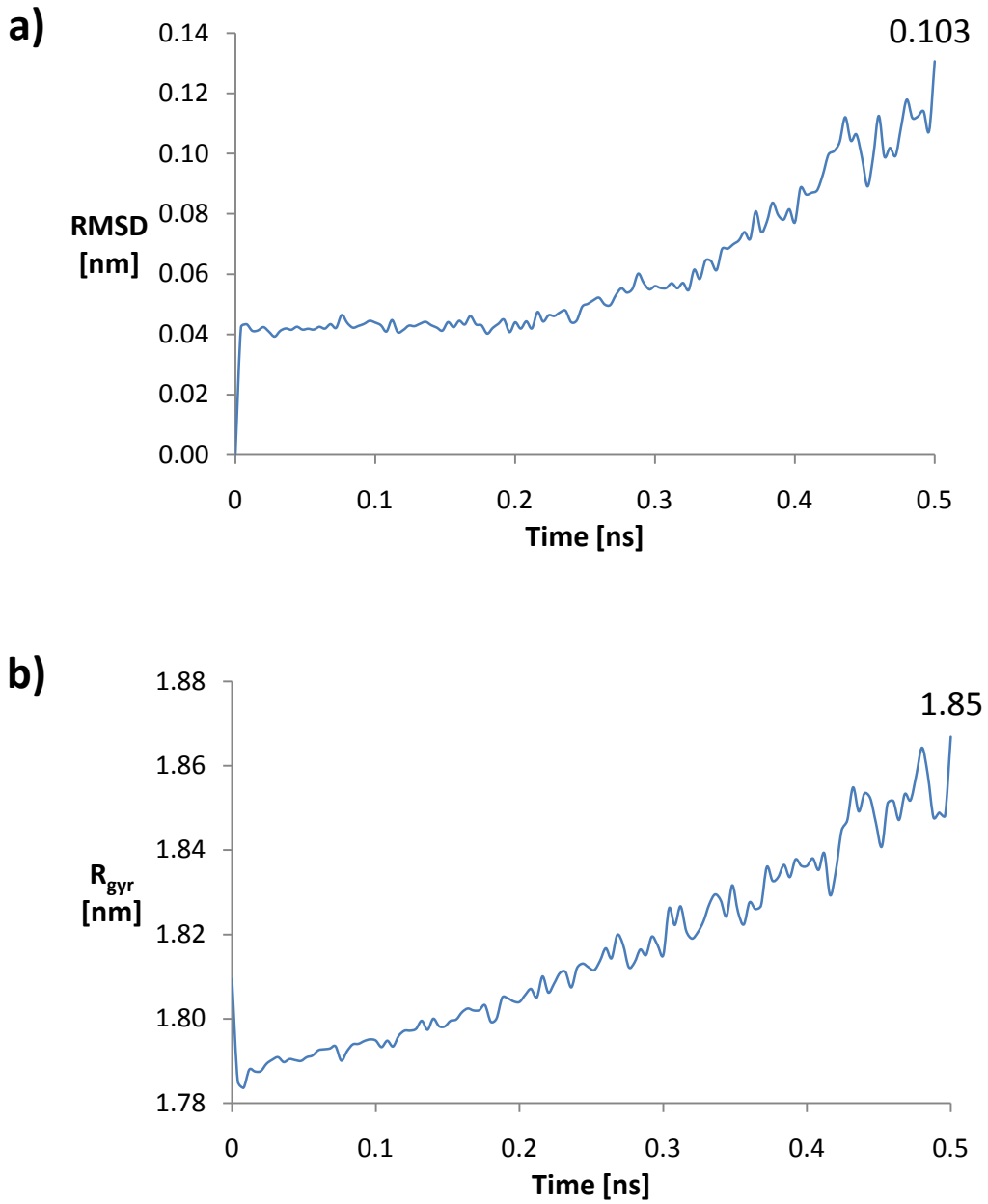

Fig. S33 Plot of various stability measures of CAL-B solvated by BMIM-NO_3 over time, with a different heating pattern. The plots shown here were heated from 1 to 600K in 500ps. a) root mean square deviation, RMSD b) radius of gyration, R_{gyr}. Value shown at the end of the curve is an average over the last 100 ps.

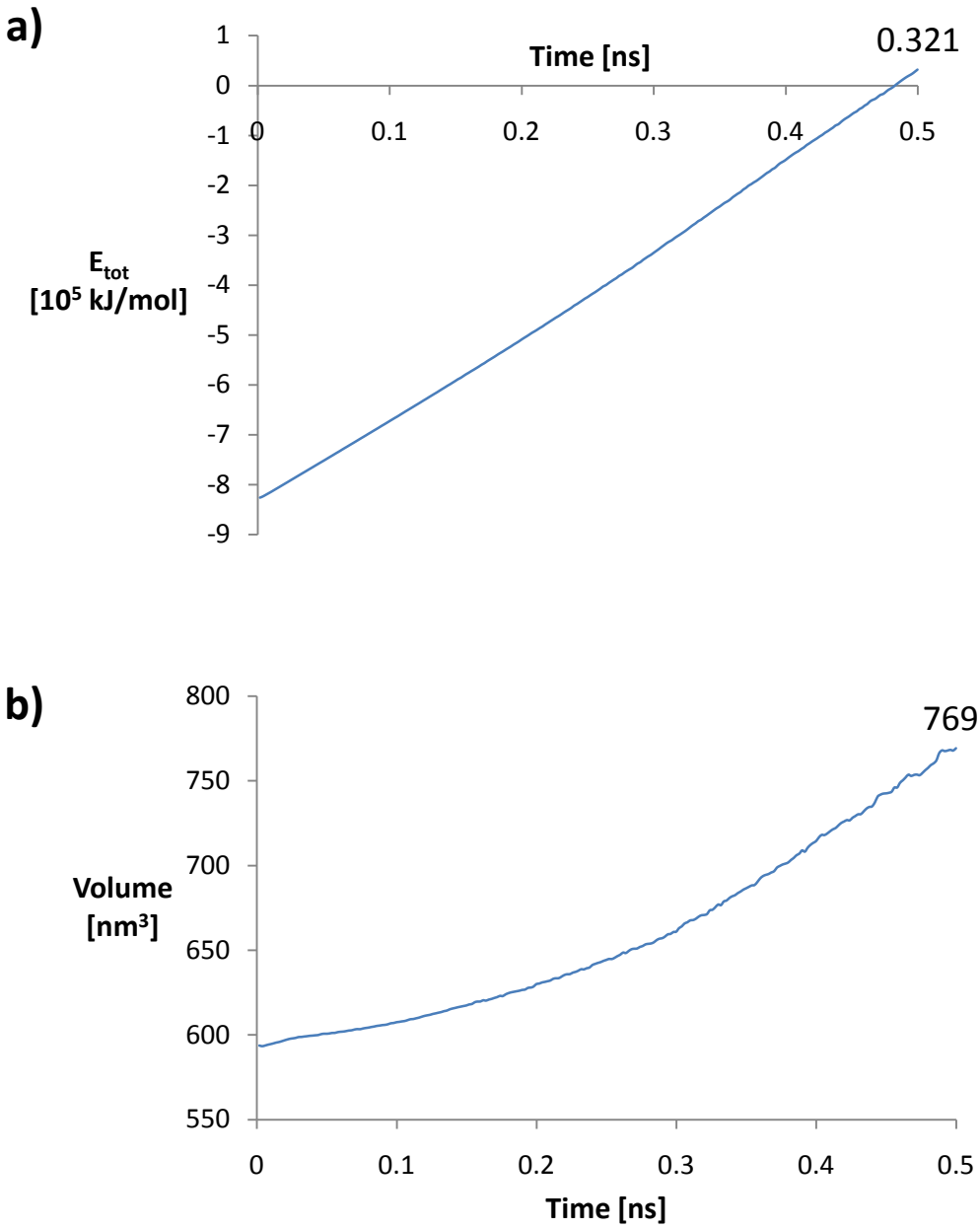

Fig. S34 Plot of various stability measures of CAL-B solvated by BMIM-NO_3 over time, with a different heating pattern. The plots shown here were heated from 1 to 600K in 500ps. a) total energy, E_{tot} b) box volume. Value shown at the end of the curve indicates the value at 5ns.

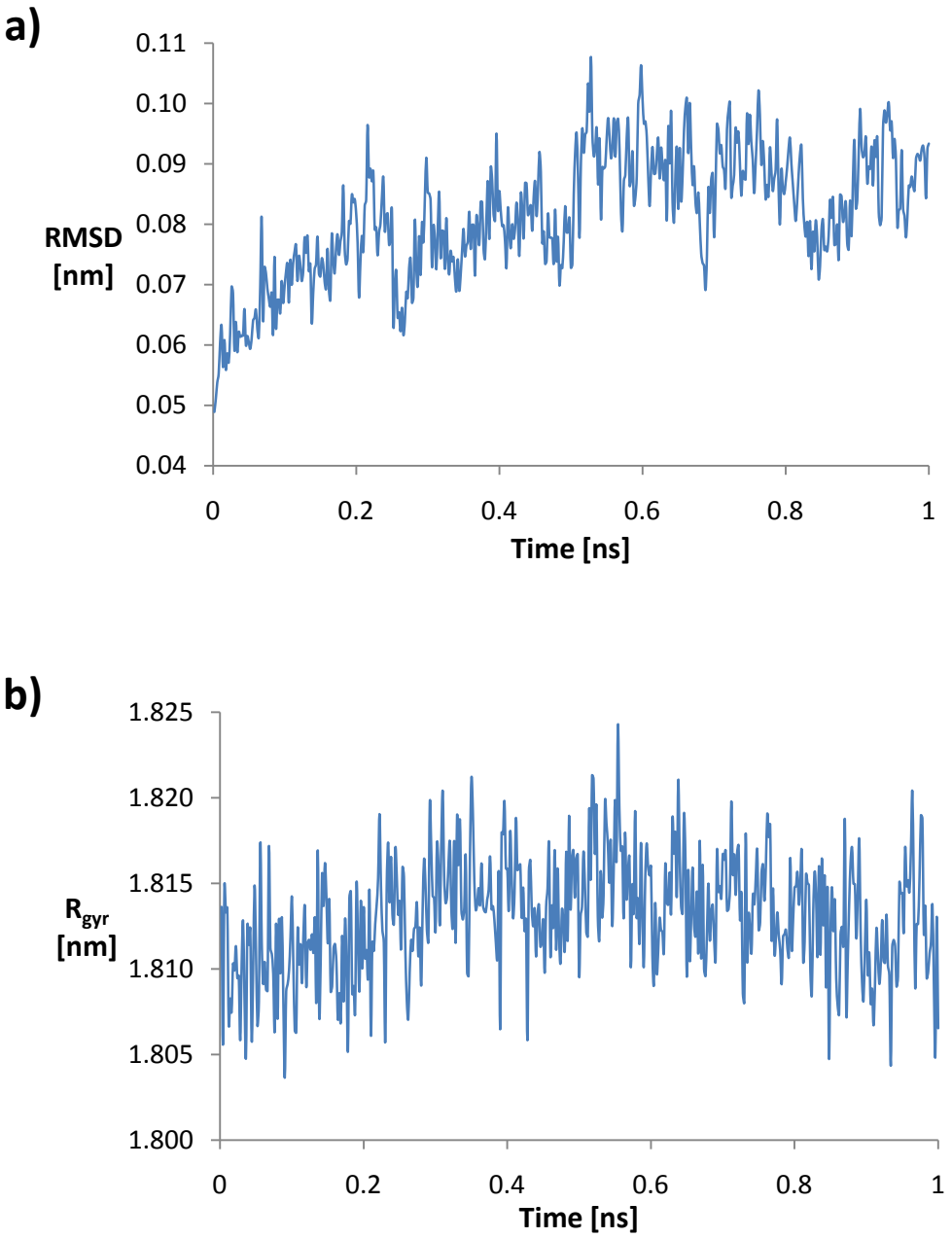

Fig. S35 Plot of a) root mean square deviation, RMSD, and b) radius of gyration, R_{gyr}, of CAL-B solvated by water over 1ns at 300K.

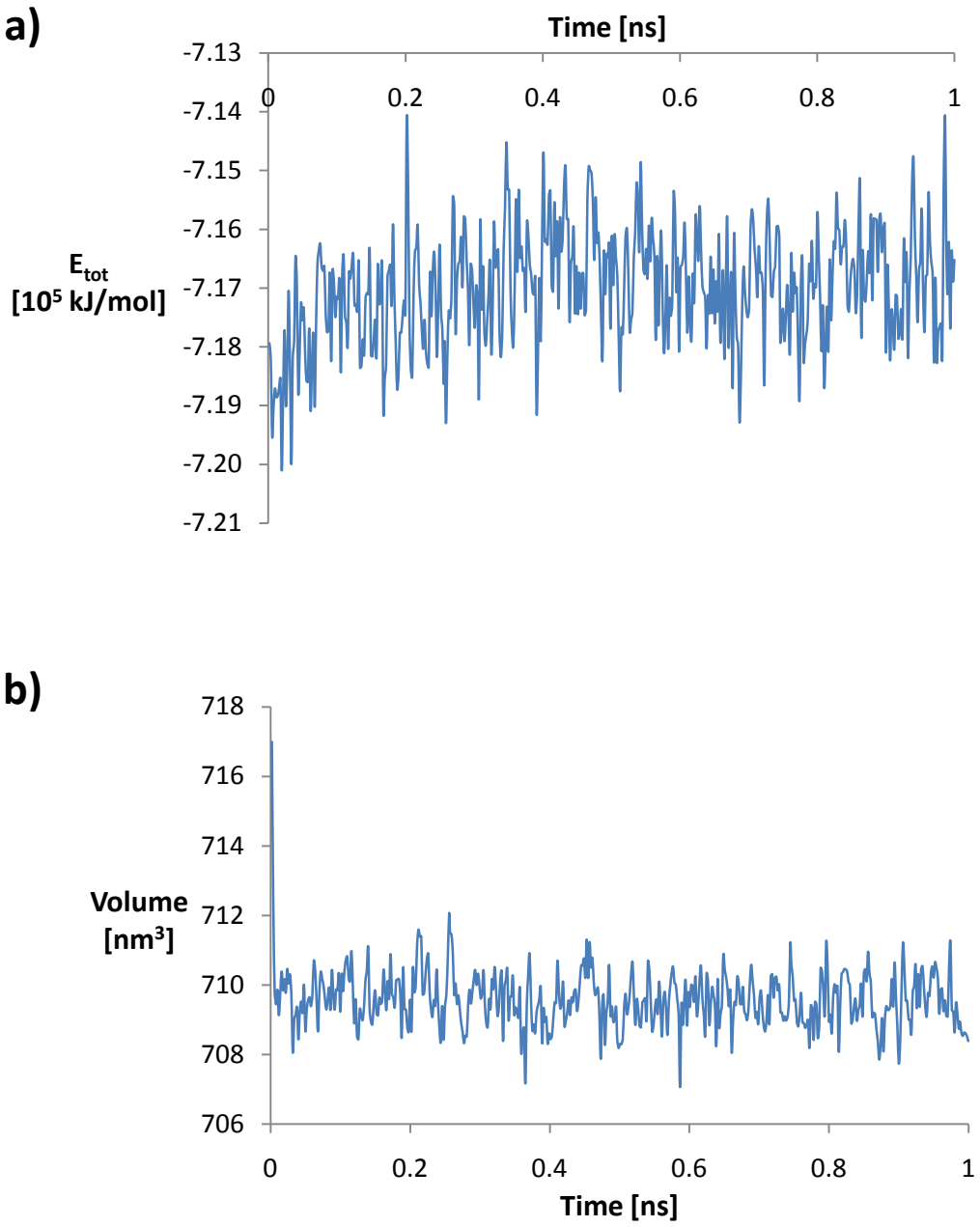

Fig. S36 Plot of a) total energy, E_{tot}, and b) box volume, of CAL-B solvated by water over 1ns at 300K.